Double-stranded RNAs targeting *Sphaerulina musiva* silence *DCL* but not *CYP51 in vitro*, and fail to confer resistance to canker in transgenic poplar

Michael I. Gordon[1], Cathleen Ma[2], Posy E. Busby[3], Steven H. Strauss[2*], and Jared M. LeBoldus [3,4*]

[1]The Department of Molecular and Cellular Biology, Oregon State University, Corvallis, OR 97331, U.S.A.

[2]The Department of Forest Ecosystems and Society, Oregon State University, Corvallis, OR 97331, U.S.A.

[3]The Department of Botany and Plant Pathology, Oregon State University, Corvallis, OR 97331, U.S.A.

[4]The Forest Engineering, Resources and Management Department, Oregon State University, Corvallis, OR 97331, U.S.A.

*Corresponding Authors: jared.leboldus@oregonstate.edu and steve.strauss@oregonstate.edu

Funding: United States Department of Agriculture Biotechnology Risk Assessment Research Grant #2019-33522-30199 to JL, PB and SS. The Department of Energy -

Oak Ridge National Laboratory; Secure Ecosystem Engineering and Design Science Focus Area to JL (CW54158).

Abstract

Host-induced gene silencing (HIGS) is a common method for engineering plant protection against pathogens, although success requires double-stranded (dsRNA) uptake mechanisms that may not be present in all fungi. We explored HIGS in transgenic poplar to study and control *Sphaerulina musiva*, the cause of Septoria stem canker disease. HIGS transgenic poplars expressing dsRNA that targeted either or both *S. musiva CYP51* and *DCL* were developed and screened for resistance to stem canker disease in two greenhouse inoculation trials. While differences in resistance between transgenic lines and wild-type controls were not detected, there was a correlation between greenhouse-expressed disease resistance and transgene expression among HIGS lines targeting *S. musiva DCL.* To evaluate the likelihood that HIGS or spray-induced gene silencing might be effective under some conditions, concurrent with greenhouse screening we studied: 1) *S. musiva's* capacity for uptake of environmental dsRNA; 2) effects of *in vitro* silencing of *CYP51* and *DCL* on fungal growth and target transcript abundance; and 3) persistence of dsRNA in culture. Uptake of fluorescently tagged dsRNA was not detected with confocal imaging. In dsRNA-treated cultures, fungal growth inhibition was not detected, and RNA was rapidly degraded. Of the five target transcripts tested after dsRNA treatment, only DCL1 had reduced expression. Knockdown of *DCL1* along with the enhanced resistance among high-expressing HIGS events targeting *DCL* suggests some HIGS may have been observed. Further determination of the factors limiting dsRNA uptake by *S. musiva* are needed to determine if HIGS can be an effective technology for limiting stem canker.

Keywords: host-induced gene silencing, HIGS, Septoria canker, dsRNA uptake, Sphaerulina musiva

Introduction

Hybrid poplars are important sources of fiber and lumber (Dickmann *et al*. 2001). Productivity of short rotation plantations is threatened by Septoria leaf spot and stem canker disease caused by the ascomycete fungus *Sphaerulina musiva* (syn. Septoria *musiva*) (Ostry and McNabb 1985; Newcombe and Ostry 2001; Feau *et al*. 2010). *S. musiva* is a hemibiotroph that infects both foliar and woody tissues through natural openings such as stomata, lenticels, and petiole junctions (Weiland and Stanosz 2007; Qin and LeBoldus 2014). Colonization by fungal hyphae is restricted to the apoplast where subsequent transition to necrotrophy gives rise to canker and leaf spot symptoms (Abraham *et al*. 2019). While leaf spots lead to premature defoliation and reduced photosynthetic capacity, stem cankers pose the more significant threat to plantations as cankers girdling the vascular tissue increase the risk of wind-induced stem breakage and tree mortality (Bier 1939; Waterman 1954; Ostry and McNabb 1985; Feau *et al*. 2010). Several studies have noted failure of hybrid plantations by Septoria canker (Ostry and McNabb 1985; Lo *et al*. 1995; Weiland *et al*. 2003; LeBoldus *et al*. 2009). For example, in a mixed-hybrid *Populus* plantation in Michigan, 86% of trees had Septoria cankers five years after planting, and 69% had broken tops two years later (Ostry *et al.* 1989).

Western cottonwood (*Populus trichocarpa* Torr. and Gray) is a naive host to *S. musiva* and generally lacks resistance (Muchero *et al*. 2018). *Populus* hybrids with *P. trichocarpa* parents carry dominant susceptibility and as a consequence the progeny of many desirable *P. trichocarpa* crosses cannot be grown in areas with high disease pressure (Newcombe and Ostry 2001). Genetic resistance has long been considered the best way to manage this disease; however, breeding programs can take several years to develop resistant cultivars (Ostry 1987). Transgenic approaches leading to heritable resistance have the potential to be developed more quickly, and these efforts can complement conventional approaches with novel traits introgressed into site-adapted cultivars (National Acadamies of Sciences, Engineering, and Medicine 2019; Newhouse and Powell 2021, LeBoldus et al. 2024).

Host-induced gene silencing (HIGS) has become a commonly studied method for engineering plant protection against pathogens and pests using genetic engineering methods (Koch and Wassenegger 2021). HIGS takes advantage of widely conserved RNA interference (RNAi) mechanisms present in most eukaryotes (Shabalina and Koonin 2008). RNAi refers to the process of post-transcriptional gene silencing (PTGS) of specific messenger RNA (mRNA) that is mediated by small RNA (sRNA) with complementary sequences (Hammond *et al*. 2001). In HIGS, the sequence of the silencing RNA is carefully selected to determine which genes can be effectively silenced. The sRNAs that trigger RNAi are double stranded RNA (dsRNA) and are processed by dicer-like proteins (DCL) into small interfering RNAs (siRNAs) that are ~ 21-24 bp in length. siRNAs then complex with argonaute proteins (AGO) that selectively remove one strand and use the other to form an RNA-induced silencing complex

(RISC). RISC then silences (i.e., knocks-down) mRNA with complementary sequence to the siRNA by transcript cleavage or translational inhibition. RNAi also includes processes of transcriptional gene silencing (TGS) whereby siRNA and AGO guide a DNA methyltransferase as part of an RNA-induced transcriptional silencing complex (RITS) to epigenetically silence transcription of genes with complementary sequences (Bhattacharjee *et al*. 2019). Most HIGS studies focus on PTGS though it's unclear if PTGS contributes more to target gene silencing in HIGS applications than does TGS (Karimi and Innes 2022).

Since the term HIGS was coined by Nowara *et al.* (2010) the method has been applied against viruses, insects, and nematodes in diverse host species (Koch and Wassenegger 2021). An early and influential example of HIGS was reported by Koch *et al.* (2013). They demonstrated resistance to *Fusarium graminearum* in both barley and *Arabidopsis* by using HIGS to knock-down the same genes targeted by azole fungicides. By expressing dsRNA complementary to all three paralogs of *F. graminearum* cytochrome P450 lanosterol C14α-demethylase genes (*CYP51*), they demonstrated the potential of HIGS to limit dependence on fungicides. In another study, Wang *et al.* (2016) demonstrated that *B. cinerea* RNAi genes (*DCL1 and DCL2*) were also effective HIGS targets. These genes are effective targets in *B. cinerea* because they are essential for the biogenesis of siRNA effectors that are trafficked into plants to silence host immunity genes (Weiberg *et al*. 2013; Wang *et al*. 2016). This phenomenon is known as cross-kingdom RNAi (ckRNAi) and has been observed in the opposite direction with plants generating siRNA to silence fungal genes (Cai *et al*. 2018).

Observations of ckRNAi and HIGS both demonstrate that at least some fungi carry mechanisms for uptake of plant-derived dsRNA.

RNAi-mediated control of pest and pathogens has also been demonstrated by spraying dsRNAs directly onto plants (Koch *et al*. 2016; Wang *et al*. 2016; Rank and Koch 2021). Known as spray-induced gene silencing (SIGS), this strategy can be as effective as HIGS and has the potential to offer the most pathogen-specific fungicides ever developed (Koch *et al*. 2019; Hough *et al*. 2022). SIGS may eventually be applied more than HIGS as it skirts the need for host transformation and public acceptance of genetically modified organisms. SIGS studies have demonstrated additional routes by which fungi take up dsRNA. In addition to uptake from HIGS plants, some fungi can also take dsRNA directly from the environment (Wang *et al*. 2016; McLoughlin *et al*. 2018; Qiao *et al*. 2021). With SIGS, it is thought that fungi take up dsRNA both from the leaf surface, and from plant tissues after dsRNA has first been absorbed and translocated within the plant (Niu *et al*. 2021). The mechanisms of fungal uptake continue to be studied (Karimi and Innes 2022).

While RNAi is nearly ubiquitous in fungi (Nakayashiki *et al*. 2006), the ability to take up dsRNA—either from the host or the environment—may be much less common. Kettles *et al*. (2019) have shown that the wheat pathogen *Zymoseptoria tritici* may not be amenable to HIGS and SIGS. *In vitro* RNAi and HIGS against essential *Z. tritici* genes was inefficient at reducing fungal growth and virulence respectively. They also showed a lack of uptake of fluorescently tagged dsRNA in culture using live imaging. In a similar

approach, Qiao *et al*. (2021) found variable environmental dsRNA uptake efficiencies among five fungi. When HIGS was tried against the same fungi, the only species whose virulence was not attenuated by HIGS was the one fungus with the least efficient uptake *in vitro* (*Colletotrichum gloeosporioides*). It therefore appears that dsRNA uptake mechanisms critical for HIGS and SIGS are not present in all fungi.

The goal of this study was to see if HIGS-based resistance to *S. musiva* stem canker could be engineered in *P. trichocarpa*. Gene targets *CYP51* and *DCL* were the *S. musiva* homologs of gene targets found effective with HIGS against *B. cinerea* and *F. graminearum* (Koch *et al*. 2013; Wang *et al*. 2016). Existing transcriptomics for *S. musiva* (Muchero *et al*. 2018) show that *S. musiva* core RNAi genes (dicer-like, argonaute, and RNA-dependent RNA polymerase) are actively transcribed during early stages of infection and suggest functioning RNAi. To our knowledge, this is the first report of HIGS applied in an angiosperm forest species against a fungal pathogen.

Materials and Methods

ID of gene target homologs

S. musiva has one cytochrome P450 lanosterol C-α-demethylase gene (*CYP51*, SEPMUDRAFT_151286) that shares 60.3% identity with *Fusarium graminearum CYP51-B* (FGSG_01000) targeted by Koch *et al*. (2013). Unlike *F. graminearum* which has three *CYP51* copies (Liu *et al*. 2011), *S. musiva* has only one clear homolog. Without a known phenotype for *CYP51* in *S. musiva*, we opted to target two related

genes that could possibly provide functional redundancy. The protein sequence for *S. musiva CYP51* was used to identify two homologous genes based on analysis of shared domains and structural predictions in Phyr2, and phylogenetic trees built from a jackHMMER search. Homologs *CYP6A1* (SEPMUDRAFT_149948) and *CYP61* (SEPMUDRAFT_147259) were also targeted by our RNAi constructs.

S. musiva has two dicer-like (*DCL*) copies: *DCL-1* (SEPMUDRAFT_72068) shares 34.0% identity with *Botrytis cinerea DCL-1* (BCIN_12g06230), and *S. musiva DCL-2* (SEPMUDRAFT_136183) shares 32.4% identity with *B. cinerea DCL-2* (BCIN_14g03910)—both of which were targeted by Wang *et al.* (2016). A similar search for homologs of *DCL1* and *DCL2* (SEPMUDRAFT_72068, SEPMUDRAFT_136183) failed to identify additional genes suspected to encode functional redundancy.

To ensure the relevance of target genes during infection, the expression of all five *S. musiva* gene targets were checked against published transcriptomes (Dhillon *et al*. 2015). The protein sequences of these *S. musiva* gene targets, and those of their homologs targeted in other HIGS studies, were aligned using MAFFT (Katoh and Standley 2013) and the conserved amino acid sites were used to generate neighbor-joining trees (Fig. S1).

RNAi constructs

RNAi constructs for *in vitro* RNAi and HIGS transgenics were designed using siRNA Finder version siFi21_1.2.3-0008 (Lück *et al*. 2019). Gene target fragments, ranging in size between 251-315 bp, from within the target mRNA coding sequence were selected

based on both the predicted density of high efficiency siRNAs (Lück *et al*. 2019), and lack of off-target silencing against *Populus trichocarpa* v3.1 transcripts. Stacked RNAi constructs for like gene targets were synthesized and inserted into backbones p9U10-RNAi and p6U10-RNAi by DNA Cloning Service (Hamburg, Germany). p9U10-RNAi-*Sm-CYP51* targets *S. musiva CYP51* and two of its homologs while p6U10-RNAi-Sm-DCL targets both *S. musiva DCL* genes. p9U10-RNAi-GUS targets *E. coli* beta-glucuronidase (*GUS)* and serves as a non-specific double stranded RNA (dsRNA) control (Fig. S2).

S. musiva culture

Sphaerulina musiva isolate MN-14 (Dunnell and LeBoldus 2017) was used for all experiments due to its prolific sporulation in culture and strong symptom development in *Populus trichocarpa* clone SLMB-28-1. MN-14 was routinely cultured on KV-8 agar (2 g calcium carbonate, 20 g agar, 820 mL deionized water, and 180 mL V-8 vegetable juice (Campbell Soup Company, Camden, NJ, USA)) under continuous lighting for one to two weeks to induce sporulation. Conidia were harvested and quantified by flooding plates with sterile water, scraping mycelia, and counting cells with a haemocytometer.

In vitro RNAi

dsRNA

Synthetic double stranded RNAs (dsRNA) used to assay target gene knock-down, growth inhibition, and dsRNA stability were sourced from Greenlight Biosciences (Lexington, MA) (Fig. S3). *Sm-CYP51* dsRNA (891 bp), *Sm-DCL* dsRNA (645 bp), and *GUS*-dsRNA (594 bp) are identical in sequence to dsRNAs produced by our RNAi

constructs (Fig. S2) minus the restriction sites added between stacked gene fragments, and the addition of 15 bp internal transcribed spacer (ITS) sequences at both ends.

Growth inhibition

To quantify inhibitory effects of fungicide and dsRNAs on fungal growth, we used the *in vitro* assay described by Koch *et al*. (2013). Because azole fungicides interfere with CYP51, we treated *S. musiva* with increasing concentrations of Tebuconazole (Orius® 20AQ, Makhteshim Agan of North America) to suggest whether RNAi against *CYP51* might also work to limit growth. *S. musiva* cells treated with Tebuconazole or dsRNAs *Sm-CYP51*, *Sm-DCL*, or *GUS* control were assayed for growth inhibition in microliter plates using optical density (OD600) as a proxy for growth. Wells containing 10^5 conidia, dsRNA (250, 500 or 1000 ng), and 0.8% w/v potato dextrose broth (PDB) in a total volume of 200 µl were cultured at room temperature in the dark for 48 hours before OD600 was measured on a Tecan Spark 10M microplate reader in technical triplicate. Amounts of dsRNA were consistent with those previously reported (Koch *et al*. 2013; Wang *et al*. 2016; Kettles *et al*. 2019). Plate readings at time zero were used as blanks to subtract background absorbance. Technical replicate OD600 readings were averaged and normalized to average OD600 values for growth of untreated cell controls. One-tailed t-tests were used to test for reductions in mean response of three independent experiments relative to the control. *Post hoc* power analysis using observed response variation was used to suggest the detectable effect size (one-tailed t-test, n=3, alpha= 0.05 and power =0.80).

dsRNA longevity in culture

In microwell plates, 10^5 *S. musiva* conidia were cultured in 0.8% (w/v) potato dextrose broth containing 1 µg *GUS*-dsRNA in a total volume of 100 µl. Cultures were incubated at room temperature in the dark. Supernatants were harvested every 12 hours for 72 hours and stored at -80°C until all samples were collected. Supernatants from the entire 72-hour period were then thawed, combined with 10 µl gel loading buffer, and run through large format 1% agarose gels (wells ~150 µl, 100 v for 50 min) to make qualitative evaluations of band size and intensity—compared to sterile control wells that received only broth and dsRNA. An 8-day old culture of *S. musiva* in 0.8% potato dextrose broth was filter sterilized (0.2 µm) and used in place of fungal spores in the above assay. Sterility of the filtrate was checked on KV-8 agar. The same culture filtrate treated with proteinase K (New England Biolabs #P8107S) (30 units/ml filtrate, 37° for 1 hour) was also used in place of fungal spores in the above assay.

Knock-down of fungal gene targets

S. musiva was cultured in KV8 broth (pH 7) with $2x10^4$ conidia/ml and 100 ng/µl dsRNA in flasks shaken at 200 RPM in the dark at room temperature. Cultures were treated with either *Sm-CYP51* dsRNA, *Sm-DCL* dsRNA, or *GUS* control dsRNA. After 24, 36, and 48 hours, mycelia were vacuum filtered, rinsed with sterile water, added to 2 ml lysing tubes (MP bio lysing matrix I, #116918050-CF), frozen on liquid nitrogen, dry homogenized for 20 seconds at 6 m/s (Savant FastPrep FP120 Cell Disruptor), returned to liquid nitrogen for 2 min, and dry ground two additional times. Total RNA extraction with Trizol, DNase treatment, reverse transcription, and qPCR were performed as noted in transgene expression methods below. Relative expression was normalized to fungal

reference gene actin (SEPMUDRAFT_147624). Two-tailed t-tests were used to test for differences in mean dCts relative to the control. Primers used for relative expression targeted regions of transcripts that did not overlap with dsRNA constructs, therefore any residual dsRNA treatment captured during total RNA isolation and present in cDNA libraries could not be amplified during qPCR (Table S2.1). Independent experiments for each timepoint were repeated at least three times.

Assessment of tagged dsRNA uptake

The ability of *S. musiva* isolate MN-14 to uptake exogenous siRNA was assessed using BLOCK-iT™ Alexa Fluor™ Red Fluorescent Control (Invitrogen #14750100). For uptake of long dsRNA, a 741 bp dsRNA complementary to enhanced green fluorescent protein (*eGFP*) was transcribed using cy3-UTP (APExBIO #B8330) along with HiScribe® T7 High Yield RNA Synthesis Kit (New England Biolabs #E2040S). Microscope slides were coated with 1% agar containing 0.1% (w/v) potato dextrose broth (BD Difco #254920) and prepared with simultaneous and overlapping applications of 500 conidia applied in 5 µl, and either 500 ng dsRNA or 500 ng siRNA in 5 µl. Controls were similarly treated with either 5 µl water or 20 µM cy3-UTP. Slides were incubated in a moist chamber in the dark at room temperature for either 12, 24, or 48 hours and then treated with 75 U micrococcal nuclease at 37 °C for 30 min (New England Biolabs # M0247S) before viewing on a ZEISS LSM 780 NLO confocal microscope (Confocal Microscopy Facility of the Center for Quantitative Life Sciences at Oregon State University). *Botrytis cinerea* spores treated as above served as a positive control for dsRNA uptake (Wang et al. 2016). The *B. cinerea* isolate used in this study was isolated from *P. trichocarpa* leaves in Corvallis, OR and identified by its ITS2 sequence. Laser intensity for red fluorescence

(excitation/emission 555/565 nm) was first set with the cy3-dsRNA treated *B. cinerea* cells and the same settings were used for all other treatments. Experiments at the 12-hour timepoint were repeated three times.

HIGS transformations

S. musiva-susceptible *Populus trichocarpa* genotype SLMB-28-1 (Muchero *et al*. 2018) was transformed with the constructs above (Fig. S2A) using standard *Agrobacterium* methods (Ma *et al*. 2004; Song *et al*. 2006; Li *et al*. 2017). Leaf and stem explants were co-cultivated with *Agrobacterium* strain AGL1 at a concentration of 0.6-0.8 optical density. Shoots forming under hygromycin and or kanamycin selection were PCR confirmed for the full-length dsRNA transgenes. A total of 81 HIGS events were generated including 39 p9U10-RNAi-CYP51 events, 30 p6U10-RNAi-DCL events, 12 events co-transformed with both p9U10-RNAi-CYP51 and p6U10-RNAi-DCL, and six p9U10-RNAi-GUS control events.

Poplar culture

Transgenic events and *WT* controls were maintained and replicated *in vitro* on woody plant media with rooting hormone (WPM-RT). Rooted plants were acclimated to soil (SunGro Sunshine #4) in 2¼ x 3¼ inch pots (Anderson #1683) placed in sealed 1-gallon plastic bags with an 18-hour photoperiod for three weeks in a headhouse. Plants were acclimated by first opening plastic bags for one week, then pots were transferred into translucent plastic tubs with slightly opened lids in a greenhouse for two additional weeks. Lids were gradually removed over the first week. Acclimated greenhouse plants were potted in 2.5 x 10-inch Deepot cells. Plants were fertilized weekly with liquid 20-

20-20 (Harrell's # 880105-VI) at 500 ppm N. Side shoots were trimmed to encourage growth of the main stem. Plants received an 18-hour photoperiod. Fertilization was discontinued at the start of the inoculation experiments.

Greenhouse resistance screening

Trees were inoculated by spraying all stem and leaf surfaces to run-off with conidia suspended in sterile water using a spray bottle. Inoculated trees were initially covered in plastic bags and incubated in the dark for 48 hours to maintain relative humidity. The germination rate was quantified by counting spores plated on water agar for 12 hours. Symptoms developed over three weeks. Disease severity was quantified as the mean number of stem cankers formed 3-weeks post-inoculation (WPI) normalized by height in cm at time of inoculation.

The first experiment containing the initial transformants was inoculated with a $5x10^5$ conidia/ml. Line (event) level replication was five ramets and the experiment contained a total of 129 ramets that survived soil acclimation. All SLMB 28-1 trees were allowed to reach an average height of 48.7±8.86 cm before inoculation. Resistant hybrids 353 (*tremula x tremuloides)* and 717 (*tremula x alba)* were included as positive controls for resistance.

The second replicated greenhouse study saw the following modifications: (1) the inoculum dose was decreased to 10^5 conidia/ml to avoid overwhelming potential resistance, (2) ramet level replication was increased to raise experimental power, (3) events were selected to focus on four of the highest HIGS transgene expression events and two low expression events for each *S. musiva* targeting construct type (*Sm-CYP51*,

Sm-DCL, and *Sm-CYP51* + *Sm-DCL*). Trees were allowed to reach an average height of 29.22±5.06 cm prior to inoculation. Stunted ramets (< 19 cm) were removed from the analysis.

Analysis of variance (ANOVA) was used to test for effects of construct and event on disease severity (cankers/cm) with starting height included as a covariate. Dunnett's test, a multiple comparisons-corrected test for the case of comparing all treatments to a control, was used to compare all experimental treatments to the *wild type*.

Transgene expression

Relative HIGS transgene expression was measured across all HIGS transgenic events to: (1) ensure transgenes were expressed in most lines; (2) identify the highest expressing lines; (3) to focus continued resistance screening efforts on these highest expressing lines; and (4) to alleviate concerns of transgene silencing that might have prevented target gene RNAi. Reverse transcription quantitative polymerase chain reaction (RT-qPCR) was used to measure relative expression of both HIGS and marker gene transcripts produced by our RNAi constructs. Total RNA was extracted from combined leaf and stem tissues of single ramets in micropropagated culture using Trizol reagent (Invitrogen #15596) following the manufacturer's instructions. A high salt buffer (0.8 M sodium citrate and 1.2 M NaCl) was used 1:1 with isopropanol during RNA precipitation to aid in removal of plant polysaccharides. Total RNA preps were treated with Turbo DNase (Invitrogen #AM2238). Total RNA was reverse transcribed with a mix of both oligo-dT and random primers using iScript cDNA synthesis kit (Biorad#1708891) with 500 ng total RNA in 10 µl reactions. Relative transcript abundance was quantified using PowerUp™ SYBR™ Green Master Mix (Applied Biosystems #A25742) with 10 ng

cDNA as template in 10 µl duplicate reactions with forward and reverse primers at 500 nM each (Table S2.1). Expression of HIGS and marker transcripts were normalized to host reference gene elongation factor 1-beta (Potri.009G018600). Relative expression was calculated as $2^{-(dCt)}$ where dCt is difference in cycle thresholds ($Ct_{\text{gene of interest}} - Ct_{\text{reference}}$). Pearson's product-moment correlation coefficients were calculated to test for negative correlations of HIGS transgene expression and disease severity with p-values representing one-tailed tests.

Results

S. musiva is sensitive to azole fungicide

The minimum inhibitory concentration (MIC) of tebuconazole that limited visible growth was 200 nM (Fig. S4). No growth was detected at 400 nM. These concentrations are three orders of magnitude below the recommended dilute spray rate for control of foliar leaf spot pathogens (4.3 oz/100 gal or ~200 µM tebuconazole).

In vitro RNAi targeting *CYP51* and *DCL* genes does not inhibit *S. musiva* growth

To determine whether *in vitro* silencing of *CYP51* and *DCL* would impair growth, germinating conidia were treated with 891 bp *Sm-CYP51* dsRNA and 645 bp *Sm-DCL* dsRNA respectively in microwell culture. A 594 bp *GUS*-specific dsRNA served as a negative control. Growth of cells treated with either *Sm-CYP51* dsRNA or *Sm-DCL* dsRNA at any of three doses (250, 500, or 1000 ng) was not statistically different than the control treatments ($p > 0.25$) (Fig. 1). The standard deviations between replicate responses (optical density relative to untreated cells) within each of nine treatment

groups had an average of 23.0%. A *post hoc* power analysis using this variation suggested an effect size of 70.6% (growth reduction) was necessary to detect a significant difference at (alpha = 0.05).

Rapid degradation of dsRNA in both culture and culture filtrate

To measure the duration of time that full length dsRNAs remained intact and in solution under the *in vitro* conditions used above, supernatants from *GUS*-dsRNA treated microwell cultures were collected over 72 hours. Band size and intensities were qualitatively compared to control wells that received only broth and dsRNA. After 24 hours, no dsRNA band was visible in supernatant from treated culture while dsRNA bands from control wells remained intact over 72 hours (Fig. 2A). The disappearance of dsRNA over time could be explained by either extracellular dsRNA degradation, and or fungal uptake. Therefore, dsRNA was also treated with the filtrate of *S. musiva* culture to test for secretion of RNase. After culture filtrate and dsRNA were incubated together for 8 hours, dsRNA was no longer visible on a gel (Fig. 2B). To establish whether this result was due to a secreted proteinaceous nuclease, we also incubated dsRNA with culture filtrate treated with proteinase K (Fig. 2C). Contrary to the results of filtrate treated dsRNA, dsRNA treated with proteinase K treated filtrate persisted over 72 hours.

***In vitro* RNAi against *Sphaerulina musiva* results in down-regulation of one of five gene targets**

To determine whether target transcripts were silenced *in vitro*, total RNA was extracted from dsRNA treated cultures over 48 hours, and transcript abundance was measured

using RT-qPCR. Having previously observed the rapid disappearance of dsRNA treatments from solution within 24 hours (Fig. 2A), the dsRNA concentration in this experiment was increased 10-fold to ensure that dsRNA remained available for the duration of the experiment. Analysis of dsRNA remaining in culture supernatant after 48 hours on agarose gels had dsRNA bands of equal intensity to dsRNA bands of the 0-hour supernatant and suggested dsRNA was available for uptake throughout the duration of the experiment (gel not shown).

Of the three transcripts targeted by *Sm-CYP51*-dsRNA, no silencing was observed at 24, 36, or 48 hours (Fig. 3A). Of the two transcripts targeted by DCL-dsRNA, only *DCL1* expression was silenced (Fig. 3B). Knock-down was observed for *DCL1* at all three time points and ranged from 92.4% at 24 hours to 79.4% at 48 hours (*DCL1* vs. control difference in mean dCt = $3.71_{24\text{-H}}$, $3.59_{36\text{-H}}$, $2.28_{48\text{-H}}$). In contrast, the average difference in mean dCt for the other four targets at all three timepoints was -0.07±0.72 standard deviations. The average reference gene Ct was 19.3±1.0 cycles.

No detection of uptake of fluorescent dsRNA using live cell imaging

To investigate the efficiency of dsRNA uptake by *S. musiva in vitro*, we used fluorescently tagged dsRNAs with confocal microscopy (Galli *et al*. 2020; Hamby *et al*. 2020). Autofluorescence at green wavelengths was observed in germinating *S. musiva* conidia that precluded use of fluorescein in tagged dsRNA uptake experiments. Conidia were germinated on agar coated slides containing either long 741 bp cy3-labeled dsRNA complementary to *eGFP*, Alexa Fluor 555-labeled siRNA with random sequence

not complementary to any known gene, or controls cy3-UTP or water. After 12 hours, slides were treated with micrococcal nuclease to degrade extracellular dsRNA and imaged using a confocal microscope. *Botrytis cinerea* was used as a positive control for uptake as its capacity for environmental dsRNA uptake has been well established (Wang *et al*. 2016; Kettles *et al*. 2019; Qiao *et al*. 2021). As expected, fluorescence was detected in germinating *B. cinerea* spores treated with both long dsRNA and siRNA after 12 hours (Fig. 4). *S. musiva* spores; however, had no fluorescent signal detected despite a 100% germination rate at 12 hours. Similar results were also observed at 24 and 48 hours (not pictured).

No resistance detected in first greenhouse inoculation trial

To phenotype initial HIGS transformants for resistance to *S. musiva* stem canker, we inoculated trees in a greenhouse experiment (Fig. 5). No differences in mean height between constructs were detected, nor between events within constructs, that would suggest deleterious transgene or insertion effects. The mean disease severity was 0.469±0.204 cankers/cm, and all plants developed at least 2 cankers. The germination rate was 100% for this and all other greenhouse trials.

We divided canker counts by tree height to normalize counts for expected differences between taller and shorter trees. Despite this normalization, shorter trees tended to have lower normalized counts. When modeling for construct and event effects on disease severity, starting height was included as a covariate ($p < 0.02$).

We failed to reject the null hypothesis that construct had no effect on disease severity (ANOVA, $F_{(3, 100)} = 1.73$, p = *0.165*). Similarly, we failed to reject the null hypothesis that event had no effect on disease severity (ANOVA, $F_{(21, 82)} = 1.31$, *p = 0.191*). As expected, the positive controls for resistance (hybrids 353 and 717) both had lower disease severity than *WT*-SLMB 28-1 (Fig. S5) (ANOVA, $F_{(3, 100)} = 33.3$, $p = 3.10 \times 10^{-7}$). The effect sizes for the positive controls were a 72.7% (353) and a 75.3% (717) reduction in disease severity relative to *WT*. *Post-hoc* power analysis resulted in an 80% power to detect a 66.4% (delta = 0.411 cankers/cm) reduction in the mean disease severity between HIGS events and *WT*-SLMB 28-1 (Fig. S6).

Transgene expression

A wide range of HIGS transgene expression was observed among events of the same construct (Fig. 6A and 7A). For events of p9U10-RNAi-Sm-CYP51, expression ranged from 0.84±0.14 times that of the elongation factor 1-beta reference cDNA to undetectable (Fig. 6A). For events of p9U10-RNAi-Sm-DCL, expression ranged from 2.96±0.96 times that of reference to undetectable (Fig. 7A).

Relative expression was also measured for marker genes contained on the same transfer DNA (tDNA) under different promoters (Fig. 6b and 7b). Unexpectedly, no correlation was observed between relative expression of HIGS transgenes and the marker gene among p9U10-RNAi-Sm-CYP51 events (r = 0.16, p = 0.12) while a correlation to marker gene expression among p6U10-RNAi-Sm-DCL events was (r = -

0.56, $p < 0.001$) (Fig. S7). Several events with some of the highest marker expression had little to no HIGS transgene expression detected (e.g., cyp-47, Fig. 6).

HIGS resistance not detected in second greenhouse trial

A second greenhouse experiment was used to screen high HIGS transgene expression events and controls for resistance (Fig. 8). The reduced inoculum concentration used in this trial resulted in a reduced mean disease response compared to the first experiment. The overall disease severity was 0.186±0.116 cankers/cm. There were 12 plants out of 399 that failed to develop cankers. The coefficient of variation (CV) was 62.4 while the first experiment CV was 43.7. Despite the increased CV in the second experiment, the sensitivity of the experiment was improved over the first experiment. *Post hoc* power analysis given a mean sample size of n = 16 resulted in 80% power to detect a 50.9% reduction (delta = 0.119 cankers/cm) in mean disease severity relative to the observed mean for *WT* (Fig. S8). The detectable effect size was 23.3% smaller than the effect size for the first experiment (66.4%).

Again, starting height was a significant covariate when modeling construct and event effects on disease severity ($p > 0.001$). We failed to detect a statistically significant effect of construct on cankers/cm (ANOVA, $F_{(5, 392)} = 1.86$, $p = 0.101$). However, there was strong evidence that events differed in this experiment (ANOVA, $F_{(24, 373)} = 1.99$, $p = 4.21 \times 10^{-3}$). Nonetheless, multiple comparisons against *WT* failed to identify any single events that was significantly different in cankers/cm ($p > 0.130$ for all contrasts) (Fig. S8).

Significant correlation between greenhouse resistance and expression of HIGS transgenes targeting *S. musiva DCL*

Disease severity and HIGS transgene expression of p9U10-Sm-CYP51 events were not significantly correlated in both the first trial ($r = -0.17$, $p = 0.30$) and the second trial ($r = -0.21$, $p = 0.34$) (Fig. 9A,B). When including co-transformed events in the second trial, the correlation was still not significant ($r = -0.41$, $p = 0.09$). The correlation between disease severity and HIGS transgene expression among p6U10-Sm-DCL events was not significant ($r = -0.48$, $p = 0.17$) (Fig. 9C); however, when including co-transformed events, a significant correlation was detected ($r = -0.55$, $p = 0.03$).

Discussion

For HIGS to potentially inhibit a fungal disease, it requires selection of target gene(s) that are lethal or essential for virulence, effective RNAi trigger selection (dsRNA sequence and length), and a suitable expression vector. It also requires host expression of a relevant dsRNA dose, host transfer and fungal uptake of dsRNA, an active fungal RNAi system, and sufficient silencing of target transcripts. When HIGS fails to inhibit disease severity, any one of these factors could be limiting. Overall, our results point to limited dsRNA uptake efficiency and variable RNAi trigger efficacy as likely reasons for a lack of resistance detected in greenhouse studies.

Gene targets

The gene targets we selected were based on results in other fungal systems; mutant studies in *S. musiva* were lacking. The decision to target *CYP51* and *DCL* was strongly influenced by the reported success of HIGS and SIGS against these gene targets in *Fusarium graminearum* (Koch *et al*. 2013) and *Botrytis cinerea* (Wang *et al*. 2016). Whether *CYP51* and *DCL1,2* are essential in *S. musiva* remains unclear. Our initial efforts to screen dsRNAs resulted in a lack of detectable growth reduction, which could mean either inefficient uptake, uptake but insufficient silencing, or uptake and silencing but a lack of growth phenotype. The sensitivity of *S. musiva* to demethylation-inhibitor fungicide suggests that inhibition of *CYP51* could be an effective strategy if sufficient RNAi silencing could be achieved. Despite many published HIGS studies showing efficacy against fungal pathogens (Koch and Wassenegger 2021), relatively few target *CYP51*. Aside from *Fusarium* species *(*e.g., *graminearum* (Koch *et al*. 2013)*, culmorum* (Koch *et al*. 2018), and *oxysporum* (Dou *et al*. 2020)), *CYP51* targeting has only been reported to be effective in one other species: *Magnaporthe oryzae* (Wang and Dean 2022). Thus, further study is needed to better understand *CYP51* function in *S. musiva*, and thus to establish if this could be an effective gene target for HIGS.

CYP51 copy number is variable among fungi and well known to positively correlate with azole fungicide resistance. To be an effective gene target for HIGS and SIGS, all functionally redundant copies need to be adequately silenced. For this reason, further identification of effective gene targets for HIGS and SIGS could focus on single-copy genes to simplify construct design. These could, for example, include key metabolic

("housekeeping") genes. Selection of genes that are moderately expressed (i.e., not too low or highly expressed) would also aid in assaying respective RNAi triggers *in vitro* with RT-qPCR (McLoughlin et al. 2018; Mosen 2022).

Targeting components of the RNAi pathway (e.g., *DCL*), when the goal is to use that pathway against the fungus, appears counter-intuitive; however, doing so is reported to affect growth and or pathogenicity in several fungi. Our evidence suggests *S. musiva DCL1* is not essential for conidial germination or mycelial growth *in vitro*. Our *Sm-DCL*-dsRNA suppressed *DCL1* expression; however, the same treatment had no effect on culture OD. It is possible that the degree of *DCL* silencing was insufficient to observe a growth phenotype. Conversely, if *DCL1* was sufficiently silenced, it's possible that any effect of silencing *DCL1* could have been masked by a functionally redundant *DCL2* that was not silenced by the RNAi trigger, despite being designed to target both copies.

Reduced vegetative growth *in vitro* due to knock-down or knock-out of fungal *DCL* genes appears to be relatively uncommon in fungi. Kettles *et al.* (2019) found no difference in growth rates of *Zymoseptoria tritici* mutants lacking core RNAi genes. Additional *DCL* mutant studies in *Valsa Mali* and *Penicillium italicum* also showed comparable *in vitro* growth rates to *WT* when cultured on rich media (Feng *et al*. 2017; Yin *et al*. 2020). *Fusarium graminearum DCL* mutants were reported to show normal vegetative development in axenic cultures in at least two studies (Son *et al*. 2017; Gaffar *et al*. 2019).

Growth phenotypes of *DCL* mutants in *Botrytis cinerea;* however, were less clear. Islam et al. (2021) found that dsRNA delivered in minicells to *in vitro* culture reduced growth, but only when targeting both *DCL1* and *DCL2*. Wang et al. (2016) claim attenuated growth of *Botrytis cinerea DCL1* and *DCL2* single and double mutants on malt extract agar; however, the evidence they present (image of unreplicated plates) lacked quantification or any measure of variation within groups (supporting figure 1a). Qin et al. (2023) generated their own *B. cinerea DCL* mutants and found no growth or morphology abnormalities relative to *WT*. He et al. (2023a) refute other conclusions of the Qin et al. (2023) study; however, they fail to address the contradictory *B. cinerea DCL* mutant growth phenotypes. One example of reduced *in vitro* growth comes from a *Colletotrichum gloeosporioides* double *DCL* mutant that showed attenuated growth compared to *DCL* single mutants and *WT* on both complete and minimal media (Wang *et al*. 2018).

Regardless of whether *DCL* affects fungal growth, several studies suggest the better reason to target *DCL* is because it is involved in the biogenesis of siRNA effectors used in cross-kingdom RNAi (Göhre and Weiberg 2023). SIGS and or HIGS against fungal *DCL* genes is reported to reduce pathogenicity of *Botrytis cinerea* (Wang *et al*. 2016), *Verticillium dahliae* (Wang *et al*. 2016), *Fusarium graminearum* (Werner *et al*. 2020), and *Penicillium italicum* (Yin *et al*. 2020). Additionally, reduced pathogenicity of mutant strains missing one or both *DCL* genes has been demonstrated in *Botrytis cinerea* (Weiberg *et al*. 2013), *Valsa mali* (Feng *et al*. 2017), *Colletotrichum gloeosporioides* (Wang *et al*. 2018), and *Penicillium italicum* (Yin *et al*. 2020).

The extent of siRNA effector use among fungi as a virulence strategy is unclear (Mahanty *et al*. 2023). One fungus that does not appear to use siRNA effectors is *Zymoseptoria tritici*, a close relative to *S. musiva* that shares a hemibiotrophic lifestyle (Kettles *et al*. 2019; Ma *et al*. 2020). Kettles et al. (2019) demonstrate that *Z. tritici* missing core RNAi genes were just as virulent on wheat as *WT* and conclude that RNAi plays a minimal role during infection. Whether or not *S. musiva DCL* is involved in siRNA effector biogenesis clearly requires further study. Generation of core RNAi gene knockouts in *S. musiva*, along with virulence assays, would be helpful in establishing the role of RNAi during infection. Specifically, pathogenicity screening of *S. musiva DCL* mutants paired with RNA sequencing could help determine if siRNA effectors used in ckRNAi contribute to virulence.

RNAi triggers: design and screening

Our two RNAi constructs targeted a total of five *S. musiva* genes, yet only one transcript was silenced *in vitro*. This result suggests at least some dsRNA was being taken up by *S. musiva* but that dsRNAs targeting the other four transcripts were not generating efficient siRNAs. Variation in silencing efficiency among siRNAs targeting the same mRNA is common (Holen 2002). One reason why only some siRNA are effective can be explained by mRNA secondary structure that limits access of the RNAi-induced silencing complex (RISC) to the target site (Shao *et al*. 2007). The design tool we used to select construct sequences does use mRNA structural predictions to determine which regions are most accessible to RISC (Lorenz *et al*. 2011; Lück *et al*. 2019). However, *in silico* structure predictions remain imperfect as they lack important information on

possible mRNA modifications that are known to influence secondary structure (Tanzer *et al*. 2019).

A study by Werner et al. (2020) also tested dsRNAs designed with the same software used here and found a mix of ineffective and potent silencing efficiencies among constructs targeting *Fusarium graminearum* genes *in vitro*. They found that tool-designed dsRNA constructs kept short (173-193 bp) to minimize non-target silencing tended to be less effective than manually selected longer sequences (658-912 bp) at triggering silencing in *Fusarium graminearum*. Longer randomly selected dsRNAs tended to provide greater numbers of efficient siRNA that led to stronger silencing. The same group found that dsRNA lengths up to 1500 bp were negatively correlated with SIGS-mediated disease resistance, which suggests dsRNA length eventually hinders fungal and or plant uptake (Höfle *et al*. 2020). The length of our dsRNAs were between 645 and 891 bp, and each target sequence within these stacked constructs were between 251 and 315 bp. Further study of single gene *S. musiva* constructs with longer sequences could determine if alternate target sites would be more efficient at triggering RNAi.

Our *in vitro* assays demonstrated the challenges with screening dsRNA triggers in pure culture. We found that the microwell axenic culture growth inhibition assay described by Koch et al. (2013) to be problematic with *S. musiva* due to secretion of RNase. Two SIGS studies suggest dsRNA degradation in *Botrytis cinerea* cultures might also be occurring as more efficient silencing was observed when dsRNA was applied every 12

hours (Song *et al*. 2018; Nerva *et al*. 2020). Conversely, single dsRNA additions at relatively low concentrations (0.5 ng/µl) have been shown to knock-down target gene expression for 96 hours in *Sclerotinia sclerotiorum* (McLoughlin *et al*. 2018). The dsRNA culture concentration used by Koch et al. (2013) to measure *in vitro* knock-down at 72 hours was nearly 150 times greater than the dose used on *Sclerotinia sclerotiorum* by McLoughlin et al. (2018). In the case of *S. musiva*, the dose used in our growth inhibition assay was 20 times the dose used by McLoughlin et al. (2018) and disappeared in culture supernatant after 24 hours, while the same dose increased by 10-fold remained for 48 hours in *S. musiva* culture. With the range of dsRNA doses reported for *in vitro* RNAi, it's unclear the degree to which higher doses reflect a need to overwhelm secreted nuclease and/or whether the range of doses reflect differences in the efficiency of dsRNA uptake and silencing (Qiao *et al*. 2021). The methods used in this study to measure dsRNA longevity in *S. musiva* culture would be useful in evaluating relative rates of extracellular dsRNA degradation among other fungi, especially those known to uptake dsRNA more efficiently.

Further *in vitro* screening of RNAi triggers against *S. musiva* might be improved with the use of RNase inhibitors. For example, we showed that proteinase K could protect dsRNA from degradation by culture filtrate. Should *S. musiva* tolerate proteinase K in culture, it might be used to protect dsRNA, and thus improve *in vitro* uptake and silencing. Additionally, various nano-carriers can protect dsRNA from nuclease and aid its uptake into plants to elicit RNAi, potentially facilitating fungal transfection (Ray *et al*. 2022). These include "BioClay" (Mitter *et al*. 2017), carbon-dots (Schwartz *et al*. 2020),

and cell penetrating peptides (Numata *et al*. 2014) among several others. Further study is needed to see if any of these formulation strategies could aid dsRNA stability and uptake in *S. musiva* culture.

Host transgene expression:resistance relationships

Dual inverted promoter constructs are generally preferred over more traditional hairpin designs because of the relative ease of cloning (Schmidt *et al.* 2012), and as desired gave a wide range of transgene expression among the HIGS events. This style of construct has been effective in inducing HIGS in *Arabidopsis* and barley (Koch *et al.* 2013) and has also been shown to be as effective as hairpin designs in knocking down transgenes (GUS) in *Nicotiana tabacum*, or endogenous genes in hybrid aspen (Schmidt *et al.* 2012). Although no resistance was detected in greenhouse trials, transgene expression profiling provided assurance that the dual inverted promoter constructs were expressed and that enough high expression events were challenged to adequately test HIGS against our gene targets. Correlations of HIGS transgene expression and disease severity served as another line of evidence to suggest whether HIGS could explain variation in the disease response. We hypothesized that the highest expression lines would be capable of delivering the highest dose of dsRNA, and therefore would have the highest potential for resistance. Expression of HIGS transgenes did have a significant relationship with greenhouse resistance, but only among *Sm-DCL*-expressing transgenic events, and not among *Sm-CYP51*-expressing events. The significant correlation suggests that some level of HIGS might have been active in higher *Sm-DCL*-expressing events. These events targeted *S. musiva DCL1*

and *DCL2*, the former of which showed significant knock-down *in vitro* by the same dsRNA trigger. Nonetheless, even the high expression lines did not have detectably improved resistance in our greenhouse screens. It is possible that our dsRNA constructs were inefficient or that a much higher number of lines need to be screened to find very high expressors. We conclude that HIGS was not contributing to variation in disease severity that was strong enough to detect under our experimental conditions. This may be a result of inadequate dsRNA expression, limited fungal uptake, uptake but insufficient silencing, greenhouse conditions being much more conducive to disease than might occur in field-grown trees, or targeting genes not essential to growth and pathogenicity.

The methods we used to estimate dsRNA expression among HIGS transgenic lines may not have been fully reliable measures of potential disease resistance. First, HIGS transgene expression levels represent those of ramets in *in vitro* culture and are assumed to be the same among clones acclimated to greenhouse conditions. A study of transgene expression in hybrid poplar (*Populus tremula x P. alba)* found that expression increased from *in vitro* culture to greenhouse conditions in some lines while it decreased in others (Hawkins *et al.* 2003). Instability of transgene expression has also been described for *ROLC* transgenic aspen and aspen hybrids *(P. tremula L. x P. tremuloides Michx.)* after transfer from *in vitro* conditions to greenhouse (Kumar and Fladung 2001). However, stable expression of reporter genes (*GFP* and *BAR*) in poplar has also been reported over three years in the greenhouse and in the field (Li et al. 2009). Second, our methods didn't measure dsRNA directly. Priming could occur on either sense or

antisense dsRNA precursors. The assumption is that these were present in equimolar quantities and annealing to form dsRNA. Shorter dsRNAs including siRNAs derived from host-*DCL* processing of full-length dsRNA precursors could not be amplified with this approach. The priming strategy targeted 119 and 156 bp sections of the long sense and/or antisense dsRNA precursors (p9U10-RNAi-Sm-CYP51 and p9U10-RNAi-Sm-DCL respectively). Thus, the relative expression of HIGS transgenes captured by our method is assumed to represent the cellular pool of unprocessed dsRNA, which should be a fraction of the actual dsRNA expression level that includes diced dsRNA.

Both long dsRNA and siRNA are known to contribute to HIGS, though it's unclear which contributes more to silencing (Karimi and Innes 2022). It's possible that lines with low measured dsRNA expression could have had higher siRNA expression if host DCL processing was more efficient in these lines. If this were true and siRNA contributed more to HIGS in this pathosystem, then we might expect more resistance in our "low expression" lines; however, the significant negative correlation between *Sm-DCL* dsRNA expression and greenhouse disease severity is inconsistent with this hypothesis, though both specific low and high expressors could cause strong resistance, confounding a simple linear model.

Alternate methods to measure dsRNA expression could be useful. Northern blotting and related dot- and slot-blotting that are more readily quantified remain useful techniques that could be used to validate both dsRNA and siRNA expression. Stem-loop RT-qPCR is one method capable of amplifying siRNA (Varkonyi-Gasic *et al*. 2007). However,

priming for this method is specific to individual siRNA and therefore isn't suited to amplification of the many possible siRNA that can be generated from a several hundred base pair long dsRNA. RNA-seq is another option for profiling dsRNA expression across events, although costly, and is not necessarily needed if resistance is observable to screen events for functional expression.

Fungal dsRNA uptake

Several authors have suggested dsRNA uptake as the most important success factor in either HIGS or SIGS approaches against fungi (Koch and Wassenegger 2021; Qiao *et al*. 2021; Šečić and Kogel 2021). The only evidence we found for uptake was repeated knock-down of one gene target *in vitro*. However, direct observations of uptake using fluorescently labeled dsRNA and live imaging suggest efficiency is low, and that *in vitro* knock-down may have only been observed because of the high dsRNA dose needed to overwhelm secreted RNase activity in culture. In contrast to fungi such as *B. cinerea* that are known to readily take up environmental dsRNA (Wang *et al*. 2016), uptake by *S. musiva* appears relatively inefficient. Using similar methods, Qiao et al. (2021) found a range of uptake efficiencies amongst seven fungi, where strong environmental dsRNA uptake predicted efficient target gene silencing and effective SIGS control of fungal disease. Conversely, they also found that weak uptake predicted inefficient gene silencing and SIGS-mediated disease suppression in *Colletotrichum gloeosporioides.*

Another example of inefficient environmental dsRNA uptake associated with unsuccessful RNAi-mediated disease suppression comes from Kettles et al. (2019), who report a lack of detectable uptake of fluorescently labeled dsRNA in *Zymoseptoria*

tritici, as well as no resistance mediated by virus-induced gene silencing (VIGS) against essential genes. They conclude *Z. tritici* has low potential for RNAi-mediated control. Given the relatedness of *Z. tritici* to *S. musiva*, their similar hemibiotrophic life-style, and comparable poor dsRNA uptake, these fungi may share mechanisms that reduce uptake of exogenous dsRNA. Aside from these examples in *C. gloeosporioides, Z. tritici, and S. musiva,* we are unaware of any other reports of inefficient dsRNA uptake in fungi. Uptake efficiencies for the vast majority of phytopathogenic fungi remain to be described (Wytinck *et al*. 2020). Although much research remains to be done, the publication of many successful HIGS applications may reflect the well-known, and extensively documented publication bias towards significant findings (Chong et al. 2023).

The cellular mechanisms by which fungi take up dsRNA are still being discovered and debated (Wytinck *et al*. 2020; Koch and Wassenegger 2021; Šečić and Kogel 2021; Karimi and Innes 2022; He *et al*. 2023b). Mechanisms for uptake from HIGS plants may be different than those used for uptake of environmental dsRNA. For example, if plant-produced dsRNAs exported to the extracellular space are bound by protein and or packaged in extracellular vesicles (EVs), then uptake through the fungal cell wall and membrane may work with different cell receptors and transporters than those used during the uptake of exogenous naked dsRNA—as in the case of uptake from a leaf surface or *in vitro* culture. Protection of dsRNA by bound protein or encapsulation in EVs might also protect it from nuclease degradation. It's therefore plausible that a fungus showing weak uptake of environmental dsRNA might still show sufficient dsRNA

uptake from a HIGS plant to induce RNAi. This might be the case for *Colletotrichum gloeosporioides* where one study found inefficient uptake both *in vitro* and *in planta* on SIGS treated fruits (Qiao et al. 2021) while another study reports effective HIGS disease suppression in chili and tomato (Mahto *et al*. 2020). However, the gene targets were different in the two studies.

It's not clear from our greenhouse experiments whether *S. musiva* was taking up dsRNA from HIGS plants—as would strongly be suggested if we observed resistance. Our greenhouse screening methods had a lot of variability within replicated clones (CV_1 = 43.7, CV_2 = 62.4) and thus power to detect only very large effects, such as when we compared resistance to that in non-host species. Additionally, in our greenhouse studies, inoculum conditions and plant physiology were likely much different than what would be encountered in field settings, which may have overwhelmed small effect sizes. It's therefore possible that HIGS effects might have been detected under field conditions. Nevertheless, an absence of HIGS resistance does not rule out dsRNA uptake, as uptake with ineffective RNAi trigger sequences and or gene targets could also explain this result. Further study of target gene knock-down in infected tissue, preferably both *in vitro* and *in vivo*, is needed to assess the extent of *S. musiva* uptake during host colonization.

This study represents the first known attempt to develop HIGS in a forest tree against a fungal pathogen. Our very limited ability to detect dsRNA uptake by *S. musiva,* and the

lack of detectably resistant transgenic plants produced, suggest that HIGS is unlikely to be an effective means of disease control in this pathosystem.

Acknowledgments

Many thanks to our collaborators at Greenlight Biosciences for generously providing ample dsRNA for our experiments, as well as for their invaluable technical support. Thank you to Jeff Anderson for help with experimental design. This publication was made possible in part by award number 1337774 from the National Science Foundation, *MRI: Acquisition of Confocal and Two-Photon Excitation Microscope*. The authors wish to acknowledge the Confocal Microscopy Facility of the Center for Quantitative Life Sciences at Oregon State University.

Literature Cited

Abraham, N., Chitrampalam, P., Nelson, B., Sharma Poudel, R., Chittem, K., Borowicz, P., Brueggeman, R., Jain, S., and LeBoldus, J. M. 2019. Microscopic, Biochemical, and Molecular Comparisons of Moderately Resistant and Susceptible *Populus* Genotypes Inoculated with *Sphaerulina musiva*. Phytopathology. 109:2074–2086.

Bhattacharjee, S., Roche, B., and Martienssen, R. A. 2019. RNA-induced initiation of transcriptional silencing (RITS) complex structure and function. RNA Biol. 16:1133–1146.

Bier, J. E. 1939. Septoria canker of introduced and native hybrid poplars. Can. J. Res. 17c:195–204.

Cai, Q., Qiao, L., Wang, M., He, B., Lin, F.-M., Palmquist, J., Huang, S., and Jin, H. 2018. Plants send small RNAs in extracellular vesicles to fungal pathogen to silence virulence genes. Science. 360:1126–1129.

Chong, S. W., Imberger, G., Karahalios, A., Wang, A., Burggraf, M., Louis, M., Liskaser, G. M., Bianco, A., and Peyton, P. J. 2023. The relationship between study findings and publication outcome in anesthesia research following implementation of mandatory trial registration: A systematic review of publication bias. PLOS ONE. 18:e0282839.

Dhillon, B., Feau, N., Aerts, A. L., Beauseigle, S., Bernier, L., Copeland, A., Foster, A., Gill, N., Henrissat, B., Herath, P., LaButti, K.M., Levasseur, A., Lindquist, E.A., Majoor, E., Ohm, R.A., Pangilinan, J.L., Pribowo, A., Saddler, J.N., Sakalidis, M.L., Vries, R.P. de, Grigoriev, I.V., Goodwin, S.B., Tanguay, P., and Hamelin, R. C. 2015. Horizontal gene transfer and gene dosage drives adaptation to wood colonization in a tree pathogen. PNAS. 112:3451–3456.

Dickmann, D. I., Isebrands, J. G., Eckenwalder, J. E., and Richarson, J. 2001. *Poplar Culture in North America*. NRC Research Press. https://doi.org/10.1139/9780660181455 [Accessed November 10, 2023].

Dou, T., Shao, X., Hu, C., Liu, S., Sheng, O., Bi, F., Deng, G., Ding, L., Li, C., Dong, T., Gao, H., He, W., Peng, X., Zhang, S., Huo, H., Yang, Q., and Yi, G. 2020. Host-induced gene silencing of Foc TR4 ERG6/11 genes exhibits superior resistance to Fusarium wilt of banana. Plant Biotechnology Journal. 18:11–13.

Dunnell, K. L., and LeBoldus, J. M. 2017. The Correlation Between Septoria Leaf Spot and Stem Canker Resistance in Hybrid Poplar. Plant Disease. 101:464–469.

Feau, N., Mottet, M.-J., Périnet, P., Hamelin, R. C., and Bernier, L. 2010. Recent advances related to poplar leaf spot and canker caused by Septoria musiva. Canadian Journal of Plant Pathology. 32:122–134.

Feng, H., Xu, M., Liu, Y., Dong, R., Gao, X., and Huang, L. 2017. Dicer-Like Genes Are Required for H2O2 and KCl Stress Responses, Pathogenicity and Small RNA Generation in *Valsa mali*. Frontiers in Microbiology. 8. https://doi.org/10.3389/fmicb.2017.01166 [Accessed November 10, 2023].

Gaffar, F. Y., Imani, J., Karlovsky, P., Koch, A., and Kogel, K.-H. 2019. Different Components of the RNA Interference Machinery Are Required for Conidiation, Ascosporogenesis, Virulence, Deoxynivalenol Production, and Fungal Inhibition by Exogenous Double-Stranded RNA in the Head Blight Pathogen *Fusarium graminearum*. Frontiers in Microbiology. 10. https://doi.org/10.3389/fmicb.2019.01662 [Accessed November 10, 2023].

Galli, M., Imani, J., and Kogel, K.-H. 2020. Labeling of dsRNA for Fungal Uptake Detection Analysis. Methods Mol Biol. 2166:227–238.

Göhre, V., and Weiberg, A. 2023. RNA Dialogues in Fungal–Plant Relationships. In *Plant Relationships: Fungal-Plant Interactions*, The Mycota, 5: 31–51. eds. Scott, B. Mesarich, C. Springer, Cham. https://doi.org/10.1007/978-3-031-16503-0_2 [Accessed November 10, 2023].

Hamby, R., Wang, M., Qiao, L., and Jin, H. 2020. Synthesizing Fluorescently Labeled dsRNAs and sRNAs to Visualize Fungal RNA Uptake. Methods Mol Biol. 2166:215–225.

Hammond, S. M., Caudy, A. A., and Hannon, G. J. 2001. Post-transcriptional gene silencing by double-stranded RNA. Nat Rev Genet. 2:110–119.

Hawkins, S., Leplé, J.-C., Cornu, D., Jouanin, L., and Pilate, G. 2003. Stability of transgene expression in poplar: A model forest tree species. Ann. For. Sci. 60:427–438.

He, B., Cai, Q., Weiberg, A., Li, W., Cheng, A.-P., Ouyang, S., Borkovich, K., Stajich, J., Abreu-Goodger, C., and Jin, H. 2023a. *Botrytis cinerea* small RNAs are associated with tomato AGO1 and silence tomato defense-related target genes supporting cross-kingdom RNAi. bioRxiv 2022.12.30.522274. https://doi.org/10.1101/2022.12.30.522274 [Accessed November 10, 2023].

He, B., Wang, H., Liu, G., Chen, A., Calvo, A., Cai, Q., and Jin, H. 2023b. Fungal small RNAs ride in extracellular vesicles to enter plant cells through clathrin-mediated endocytosis. Nat Commun. 14:4383.

Höfle, L., Biedenkopf, D., Werner, B. T., Shrestha, A., Jelonek, L., and Koch, A. 2020. Study on the efficiency of dsRNAs with increasing length in RNA-based silencing of the *Fusarium* CYP51 genes. RNA Biology. 17:463–473.

Holen, T. 2002. Positional effects of short interfering RNAs targeting the human coagulation trigger Tissue Factor. Nucleic Acids Research. 30:1757–1766.

Hough, J., Howard, J. D., Brown, S., Portwood, D. E., Kilby, P. M., and Dickman, M. J. 2022. Strategies for the production of dsRNA biocontrols as alternatives to chemical pesticides. Front Bioeng Biotechnol. 10:980592.

Islam, M. T., Davis, Z., Chen, L., Englaender, J., Zomorodi, S., Frank, J., Bartlett, K., Somers, E., Carballo, S.M., Kester, M., Shakeel, A., Pourtaheri, P., Sherif, S.M. 2021. Minicell-based fungal RNAi delivery for sustainable crop protection. Microbial Biotechnology. 14:1847–1856.

Karimi, H. Z., and Innes, R. W. 2022. Molecular mechanisms underlying host-induced gene silencing. The Plant Cell. 34:3183–3199.

Katoh, K., and Standley, D. M. 2013. MAFFT Multiple Sequence Alignment Software Version 7: Improvements in Performance and Usability. Molecular Biology and Evolution. 30:772–780.

Kettles, G. J., Hofinger, B. J., Hu, P., Bayon, C., Rudd, J. J., Balmer, D., Courbot, M., Hammond-Kosack, K.E., Scalliet, G., and Kanyuka, K. 2019. sRNA Profiling Combined With Gene Function Analysis Reveals a Lack of Evidence for Cross-Kingdom RNAi in the Wheat – *Zymoseptoria tritici* Pathosystem. Front. Plant Sci. 10:892.

Koch, A., Biedenkopf, D., Furch, A., Weber, L., Rossbach, O., Abdellatef, E., Linicus, L., Johannsmeier, J., Jelonek, L., Goesmann, A., Cardoza, V., McMillan, J., Mentzel, T., and Kogel, K.-H. 2016. An RNAi-Based Control of *Fusarium graminearum* Infections Through Spraying of Long dsRNAs Involves a Plant Passage and Is Controlled by the Fungal Silencing Machinery. PLOS Pathogens. 12:e1005901.

Koch, A., Höfle, L., Werner, B. T., Imani, J., Schmidt, A., Jelonek, L., and Kogel, K.-H. 2019. SIGS vs HIGS: a study on the efficacy of two dsRNA delivery strategies to silence *Fusarium* FgCYP51 genes in infected host and non-host plants. Mol Plant Pathol. 20:1636–1644.

Koch, A., Kumar, N., Weber, L., Keller, H., Imani, J., and Kogel, K.-H. 2013. Host-induced gene silencing of cytochrome P450 lanosterol C14α-demethylase–encoding genes confers strong resistance to *Fusarium* species. Proceedings of the National Academy of Sciences. 110:19324–19329.

Koch, A., Stein, E., and Kogel, K.-H. 2018. RNA-based disease control as a complementary measure to fight *Fusarium* fungi through silencing of the azole target Cytochrome P450 Lanosterol C-14 α-Demethylase. Eur J Plant Pathol. 152:1003–1010.

Koch, A., and Wassenegger, M. 2021. Host-induced gene silencing – mechanisms and applications. New Phytologist. 231:54–59.

Kumar, S., and Fladung, M. 2001. Gene stability in transgenic aspen (*Populus*). II. Molecular characterization of variable expression of transgene in wild and hybrid aspen. Planta. 213:731–740.

LeBoldus, J. M., Blenis, P. V., Thomas, B. R., Feau, N., and Bernier, L. 2009. Susceptibility of *Populus balsamifera* to *Septoria musiva*: A Field Study and Greenhouse Experiment. Plant Disease. 93:1146–1150.

LeBoldus, J.M., Lynch, S.C., Søndreli, K.L., Newcombe, G., Bennett, P.I., Muchero, W., Chen, J.-G., Gordon, M.I., Liang, H., 2024 (in press). Biotechnology and Genomic

Approaches to Mitigating Disease Impacts on Forest Health. Annual Review of Phytopathology. 62:X-X. https://doi.org/10.1146/annurev-phyto-021622-114434

Li, J., Brunner, A. M., Meilan, R., and Strauss, S. H. 2009. Stability of transgenes in trees: expression of two reporter genes in poplar over three field seasons. Tree Physiology. 29:299–312.

Li, S., Zhen, C., Xu, W., Wang, C., and Cheng, Y. 2017. Simple, rapid and efficient transformation of genotype Nisqually-1: a basic tool for the first sequenced model tree. Sci Rep. 7:2638.

Liu, X., Yu, F., Schnabel, G., Wu, J., Wang, Z., and Ma, Z. 2011. Paralogous cyp51 genes in *Fusarium graminearum* mediate differential sensitivity to sterol demethylation inhibitors. Fungal Genetics and Biology. 48:113–123.

Lo, M. H., Abrahamson, L. P., White, E. H., and Manion, P. D. 1995. Early measures of basal area and canker disease predict growth potential of some hybrid poplar clones. Can. J. For. Res. 25:1113–1118.

Lorenz, R., Bernhart, S. H., Höner zu Siederdissen, C., Tafer, H., Flamm, C., Stadler, P. and F., Hofacker, I. L. 2011. ViennaRNA Package 2.0. Algorithms for Molecular Biology. 6:26.

Lück, S., Kreszies, T., Strickert, M., Schweizer, P., Kuhlmann, M., and Douchkov, D. 2019. siRNA-Finder (si-Fi) Software for RNAi-Target Design and Off-Target Prediction. Frontiers in Plant Science. https://doi.org/10.3389/fpls.2019.01023 [Accessed November 10, 2023].

Ma, C., Strauss, S., and Meilan, R. 2004. *Agrobacterium*-mediated transformation of the genome-sequenced poplar clone, Nisqually-1 (*Populus trichocarpa*). Plant Molecular Biology Reporter. 22:311a.

Ma, X., Wiedmer, J., and Palma-Guerrero, J. 2020. Small RNA Bidirectional Crosstalk During the Interaction Between Wheat and *Zymoseptoria tritici*. Frontiers in Plant Science. 10. https://doi.org/10.3389/fpls.2019.01669 [Accessed November 10, 2023].

Mahanty, B., Mishra, R., and Joshi, R. K. 2023. Cross-kingdom small RNA communication between plants and fungal phytopathogens-recent updates and prospects for future agriculture. RNA Biology. 20:109–119.

Mahto, B. K., Singh, A., Pareek, M., Rajam, M. V., Dhar-Ray, S., and Reddy, P. M. 2020. Host-induced silencing of the *Colletotrichum gloeosporioides* conidial morphology 1 gene (CgCOM1) confers resistance against Anthracnose disease in chilli and tomato. Plant Mol Biol. 104:381–395.

McLoughlin, A. G., Wytinck, N., Walker, P. L., Girard, I. J., Rashid, K. Y., de Kievit, T., Fernando, W.G.D., Whyard, S., and Belmonte, M.F. 2018. Identification and application of exogenous dsRNA confers plant protection against *Sclerotinia sclerotiorum* and *Botrytis cinerea*. Sci Rep. 8:7320.

Mitter, N., Worrall, E. A., Robinson, K. E., Li, P., Jain, R. G., Taochy, C., Fletcher, S.J., Carroll, B.J., Lu, G.Q., and Xu, Z.P. 2017. Clay nanosheets for topical delivery of RNAi for sustained protection against plant viruses. Nature Plants. 3:1–10.

Mosen, A. M. 2022. Development of RNA silencing as a novel disease control strategy to protect pines from *Dothistroma* needle blight. Master's Thesis. Massey University, Manawatu, New Zealand.

Muchero, W., Sondreli, K. L., Chen, J.-G., Urbanowicz, B. R., Zhang, J., Singan, V., Yang, Y., Brueggeman, R.S., Franco-Coronado, J., Abraham, N., Yang, J.-Y., Moremen, K.W., Weisberg, A.J., Chang, J.H., Lindquist, E., Barry, K., Ranjan, P., Jawdy, S., Schmutz, J., Tuskan, G.A., and LeBoldus, J.M 2018. Association mapping, transcriptomics, and transient expression identify candidate genes mediating plant–pathogen interactions in a tree. Proc. Natl. Acad. Sci. U.S.A. 115:11573–11578.

Nakayashiki, H., Kadotani, N., and Mayama, S. 2006. Evolution and Diversification of RNA Silencing Proteins in Fungi. J Mol Evol. 63:127–135.

National Academies of Sciences, Engineering, and Medicine. 2019. Forest Health and Biotechnology: Possibilities and Considerations. National Academies Press. https://doi.org/10.17226/25221. [Accessed November 10, 2023].

Nerva, L., Sandrini, M., Gambino, G., and Chitarra, W. 2020. Double-Stranded RNAs (dsRNAs) as a Sustainable Tool against Gray Mold (*Botrytis cinerea*) in Grapevine: Effectiveness of Different Application Methods in an Open-Air Environment. Biomolecules. 10:200.

Newcombe, G., and Ostry, M. 2001. Recessive Resistance to Septoria Stem Canker of Hybrid Poplar. Phytopathology. 91:1081–1084.

Newhouse, A. E., and Powell, W. A. 2021. Intentional introgression of a blight tolerance transgene to rescue the remnant population of American chestnut. Conservation Science and Practice. 3:e348.

Niu, D., Hamby, R., Sanchez, J. N., Cai, Q., Yan, Q., and Jin, H. 2021. RNAs — a new frontier in crop protection. Current Opinion in Biotechnology. 70:204–212.

Nowara, D., Gay, A., Lacomme, C., Shaw, J., Ridout, C., Douchkov, D., Hensel, G., Kumlehn, J., and Schweizer, P. 2010. HIGS: Host-Induced Gene Silencing in the Obligate Biotrophic Fungal Pathogen *Blumeria graminis*. The Plant Cell. 22:3130–3141.

Numata, K., Ohtani, M., Yoshizumi, T., Demura, T., and Kodama, Y. 2014. Local gene silencing in plants via synthetic dsRNA and carrier peptide. Plant Biotechnology Journal. 12:1027–1034.

Ostry, M. E. 1987. Biology of *Septoria musiva* and *Marssonina brunnea* in hybrid Populus plantations and control of Septoria canker in nurseries. European Journal of Forest Pathology. 17:158–165.

Ostry, M. E., and McNabb, H. S. J. 1985. Susceptibility of Populus species and hybrids to disease in the north central United States. Plant Disease. 69:755-757:755.

Ostry, M. E., Wilson, L. F., and McNabb, H. S. J. 1989. Impact and control of *Septoria musiva* on hybrid poplars. General Technical Report NC-133. U.S. Dept. of Agriculture, Forest Service, North Central Forest Experiment Station. https://www.fs.usda.gov/research/treesearch/10197 [Accessed November 10, 2023].

Qiao, L., Lan, C., Capriotti, L., Ah-Fong, A., Nino Sanchez, J., Hamby, R., Heller, J., Zhao, H., Glass, N.L., Judelson, H.S., Mezzetti, B., Niu, D., and Jin, H. 2021. Spray-induced gene silencing for disease control is dependent on the efficiency of pathogen RNA uptake. Plant Biotechnology Journal. 19:1756–1768.

Qin, R., and LeBoldus, J. M. 2014. The Infection Biology of *Sphaerulina musiva*: Clues to Understanding a Forest Pathogen. PLOS ONE. 9:e103477.

Qin, S., Veloso, J., Baak, M., Boogmans, B., Bosman, T., Puccetti, G., Shi-Kunne, X., Smit, S., Grant-Downton, R., Leisen, T., Hahn, M., and van Kan, J. A. L. 2023. Molecular characterization reveals no functional evidence for naturally occurring cross-kingdom RNA interference in the early stages of *Botrytis cinerea*–tomato interaction. Molecular Plant Pathology. 24:3–15.

Rank, A. P., and Koch, A. 2021. Lab-to-Field Transition of RNA Spray Applications – How Far Are We? Front Plant Sci. 12:755203.

Ray, P., Sahu, D., Aminedi, R., and Chandran, D. 2022. Concepts and considerations for enhancing RNAi efficiency in phytopathogenic fungi for RNAi-based crop protection using nanocarrier-mediated dsRNA delivery systems. Frontiers in Fungal Biology. 3. https://doi.org/10.3389/ffunb.2022.977502 [Accessed November 10, 2023].

Schmidt, N., Merker, M., and Becker, D. 2012. Novel high-throughput RNAi vectors for plant biotechnology. Plant Breeding. 131:453–456.

Schwartz, S. H., Hendrix, B., Hoffer, P., Sanders, R. A., and Zheng, W. 2020. Carbon Dots for Efficient Small Interfering RNA Delivery and Gene Silencing in Plants. Plant Physiol. 184:647–657.

Šečić, E., and Kogel, K.-H. 2021. Requirements for fungal uptake of dsRNA and gene silencing in RNAi-based crop protection strategies. Current Opinion in Biotechnology. 70:136–142.

Shabalina, S. A., and Koonin, E. V. 2008. Origins and evolution of eukaryotic RNA interference. Trends in Ecology & Evolution. 23:578–587.

Shao, Y., Chan, C. Y., Maliyekkel, A., Lawrence, C. E., Roninson, I. B., and Ding, Y. 2007. Effect of target secondary structure on RNAi efficiency. RNA. 13:1631–1640.

Son, H., Park, A. R., Lim, J. Y., Shin, C., and Lee, Y.-W. 2017. Genome-wide exonic small interference RNA-mediated gene silencing regulates sexual reproduction in the homothallic fungus *Fusarium graminearum*. PLOS Genetics. 13:e1006595.

Song, J., Lu, S., Chen, Z.-Z., Lourenco, R., and Chiang, V. L. 2006. Genetic Transformation of *Populus trichocarpa* Genotype Nisqually-1: A Functional Genomic Tool for Woody Plants. Plant Cell Physiol. 47:1582–1589.

Song, X.-S., Gu, K.-X., Duan, X.-X., Xiao, X.-M., Hou, Y.-P., Duan, Y.-B., et al. 2018. Secondary amplification of siRNA machinery limits the application of spray-induced gene silencing. Molecular Plant Pathology. 19:2543–2560.

Tanzer, A., Hofacker, I. L., and Lorenz, R. 2019. RNA modifications in structure prediction – Status quo and future challenges. Methods. 156:32–39.

Varkonyi-Gasic, E., Wu, R., Wood, M., Walton, E. F., and Hellens, R. P. 2007. Protocol: a highly sensitive RT-PCR method for detection and quantification of microRNAs. Plant Methods. 3:12.

Wang, M., and Dean, R. A. 2022. Host induced gene silencing of *Magnaporthe oryzae* by targeting pathogenicity and development genes to control rice blast disease. Frontiers in Plant Science. 13. https://doi.org/10.3389/fpls.2022.959641 [Accessed November 10, 2023].

Wang, M., Weiberg, A., Lin, F.-M., Thomma, B. P. H. J., Huang, H.-D., and Jin, H. 2016. Bidirectional cross-kingdom RNAi and fungal uptake of external RNAs confer plant protection. Nature Plants. 2:1–10.

Wang, Q., An, B., Hou, X., Guo, Y., Luo, H., and He, C. 2018. Dicer-like Proteins Regulate the Growth, Conidiation, and Pathogenicity of *Colletotrichum gloeosporioides* from *Hevea brasiliensis*. Frontiers in Microbiology. 8. https://doi.org/10.3389/fmicb.2017.02621 [Accessed November 10, 2023].

Waterman, A. M. 1954. Septoria canker of poplars in the United States. U.S. Department of Agriculture.

Weiberg, A., Wang, M., Lin, F.-M., Zhao, H., Zhang, Z., Kaloshian, I., Huang, H.-D., and Jin, H. 2013. Fungal Small RNAs Suppress Plant Immunity by Hijacking Host RNA Interference Pathways. Science. 342:118–123.

Weiland, J. E., and Stanosz, G. R. 2007. The Histology of Hybrid Poplar Clones Inoculated with *Septoria musiva*. Plant Disease. 91:1524–1530.

Weiland, J. E., Stanosz, J. C., and Stanosz, G. R. 2003. Prediction of Long-Term Canker Disease Damage from the Responses of Juvenile Poplar Clones to Inoculation with *Septoria musiva*. Plant Disease. 87:1507–1514.

Werner, B. T., Gaffar, F. Y., Schuemann, J., Biedenkopf, D., and Koch, A. M. 2020. RNA-Spray-Mediated Silencing of *Fusarium graminearum* AGO and DCL Genes Improve Barley Disease Resistance. Frontiers in Plant Science. 11. https://doi.org/10.3389/fpls.2020.00476 [Accessed November 10, 2023].

Wytinck, N., Manchur, C. L., Li, V. H., Whyard, S., and Belmonte, M. F. 2020. dsRNA Uptake in Plant Pests and Pathogens: Insights into RNAi-Based Insect and Fungal Control Technology. Plants. 9:1780.

Yin, C., Zhu, H., Jiang, Y., Shan, Y., and Gong, L. 2020. Silencing Dicer-Like Genes Reduces Virulence and sRNA Generation in *Penicillium italicum*, the Cause of Citrus Blue Mold. Cells. 9:363.

Figure Captions

Figure 1 Growth of *S. musiva* treated with dsRNA in microwell culture

Optical density at 600 nm **(**OD600) was measured at 48 hours after treating 10^5 conidia with increasing amounts of dsRNA in a total volume of 0.2 ml potato dextrose broth. Data points represent results from three independent experiments with OD600 values for treated cells normalized by the OD600 of untreated cells from each experiment. *Sm-CYP51* and *Sm-DCL* dsRNA treatments target housekeeping genes while the control treatment was a non-specific dsRNA (*GUS*). No reductions in growth were found between cells treated with dsRNAs targeting housekeeping genes and cells treated with control dsRNA (one-sided-*t-tests, p-values* shown above brackets).

Figure 2 Persistence and stability of dsRNA in culture with *S. musiva* OR its culture filtrate

S. musiva conidia (10^5) were cultured in 1% (w/v) potato dextrose broth with 1 µg *GUS*-dsRNA in a microwell plate. Culture supernatants were collected over time and then run through an agarose gel to evaluate band size and intensities compared to control wells that received only broth and dsRNA. HPI = hours post inoculation. Controls show no sign of dsRNA degradation over the duration of the experiment. **A,** dsRNA in culture

with *S. musiva* is not detectable after 24 hours. **B,** dsRNA incubated with sterile *S. musiva* culture filtrate is not detectable after 8 hours. **C,** dsRNA persists when incubated with the same culture filtrate treated with proteinase K.

Figure 3 *In vitro* knockdown of *S. musiva* gene targets

dsRNAs treatments targeted either **A,** *CYP51* homologs (cyp51) or **B,** *DCL* homologs (dcl), with a GUS non-specific dsRNA serving as the (control) treatment. The Y-axis shows Delta Ct (dCt) for all five gene targets. Each dot within a timepoint represents an independent experiment. Red asterisks highlight significant downregulation with P-values for two-tailed t-tests shown above the brackets.

Figure 4 *In vitro* uptake of red fluorescent dsRNA

Confocal imaging of germinating *S. musiva* and *B. cinerea* conidia are shown after treatment with either cy3-*eGFP*-dsRNA, BLOCK-iT™ siRNA (Alexa Fluor™), or controls cy3-UTP or water (not pictured), all followed by MNase treatment after 12 hours. Similar results were observed at 24 and 48 hours (not pictured).

Figure 5 Resistance phenotypes of HIGS lines screened in first greenhouse experiment

Cankers/cm is the mean number of stem cankers formed three weeks post inoculation divided by plant height at time of inoculation. Bars show mean values with error bars as standard error, and dots show raw data. Unique transgenic events and controls are listed on the x-axis and color is used to show construct. *WT* (*P. trichocarpa* SLMB-28-1)

is the susceptible transformation background. Constructs CYP (p9U10-RNAi-Sm-CYP51) and DCL (p6U10RNAi-Sm-DCL) target *S. musiva* genes while *GUS* (p9U10-RNAi-GUS) is a non-specific RNAi control.

Figure 6 Transgene expression across p9U10-RNAi-Sm-CYP51 events

A, Relative expression of HIGS transgene and **B,** selectable marker. Each bar represents the average of two biological replicates with error bars denoting standard error. Events labeled cyp are single transformants while c+d were co-transformed with p6U10-RNAi-Sm-DCL.

Figure 7 Transgene expression across p6U10-RNAi-Sm-DCL events

A, Relative expression of HIGS transgene and **B,** selectable marker. Each bar represents the average of two biological replicates with error bars denoting standard error. Events labeled DCL are single transformants while c+d were co-transformed with p9U10-RNAi-Sm-CYP51.

Figure 8 Resistance phenotypes of HIGS lines screened in second greenhouse experiment

Bars show mean number of stem cankers formed three weeks post inoculation, normalized by plant height at time of inoculation. Raw data is overlaid as dots. Unique transgenic events and controls are listed on the x-axis and color is used to show construct and control groups. For constructs cyp, dcl, and cyp+dcl, events are ordered left to right from high to low expression of HIGS transgenes as measured by RT-qPCR.

WT (*P. trichocarpa* SLMB-28-1) is the susceptible transformation background. NTE = non-transgenic escape with line numbers representing independent regenerated shoots that escaped selection. Constructs cyp (p9U10-RNAi-Sm-CYP51) and dcl (p6U10RNAi-Sm-DCL) target *S. musiva* genes while GUS (p9U10-RNAi-GUS) is a non-specific RNAi control.

Figure 9 Correlation of greenhouse resistance phenotypes with HIGS transgene expression

Mean resistance phenotypes (cankers/cm) from greenhouse inoculations in relation to mean relative expression of HIGS transgenes. Dots are unique transgenic events and color shows which *S. musiva* targeting construct(s) they contain. Pearson's correlation coefficients and p-values are given for both single transformants only, and for combined single and co-transformed events (blue). **A,** Correlation among p9U10-Sm-CYP51 events in the first trial. **B,** Correlation among p9U10-Sm-CYP51 events in the second trial. **C,** Correlation among p6U10-Sm-DCL events in second trial.

Supplementary Material

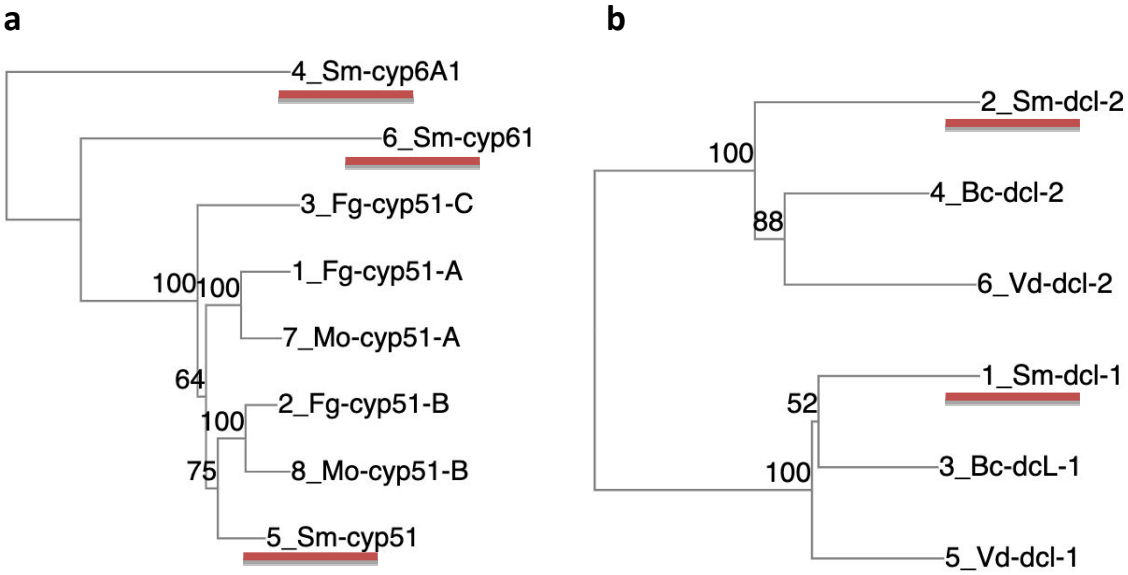

Supplementary Figure S1. Phylogenetic trees of selected *S. musiva* gene targets with homologs from other HIGS studies. Protein sequences were aligned using MAFFT (Katoh and Standley 2013) and conserved amino acids were used to generate neighbor joining trees. Red underlines show *S. musiva* genes targeted in this study. **A,** Tree showing *S. musiva* cytochrome p450 lanosterol C-a-demethylase (*CYP51*) relationship to orthologs for two fungi whose virulence is reported to have been attenuated by HIGS against *CYP51* genes. **B,** A similar tree for *S. musiva* dicer-like (*DCL*) genes. Sm = *Sphaerulina musiva*, Bc = *Botrytis cinerea*, Mo = *Magnaporthe oryzae*, Fg = *Fusarium graminearum*, Vd = *Verticillium dahliae*. Numbers at tree nodes are bootstrap values.

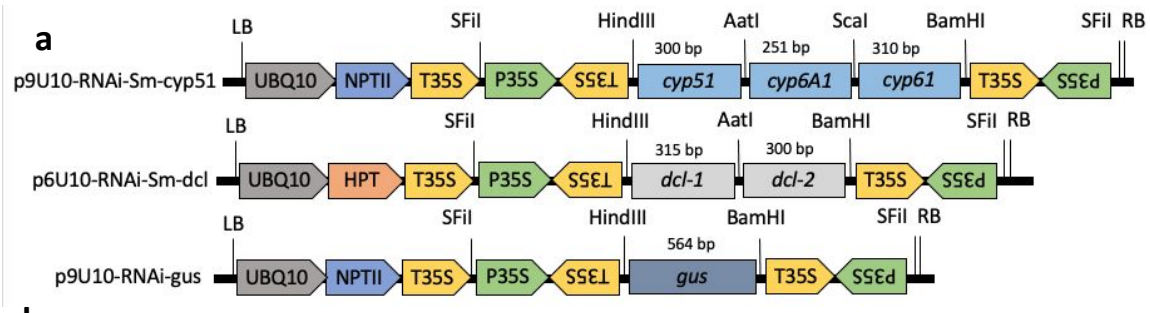

b

p9U10-RNAi-Sm-CYP51

CYP51

TTCTCCGCCTCGCCACCCGCCCCGACATTCAAGACGAGCTCGTCCAAGAGCAAAAGGACGTGCTCGGTGTCAATCCCGACGGCACTATCAAAGATGTCAGCT
ACGAAAATCTCTCCAAACTCACCCTCCTCGGCCAAGTCGTCCGAGAGACGCTCCGCATCCACGCCCCAATCCACTCCATTCTCCGCAAAGTCAAATCCCCCAT
GCCCGTCGAAGGCACTCCTTACGTGATTCCCACCACGCACTCTCTCCTCGCCGCCCCCGGGGCCACGAGCCGAATGGATGAACACTTTCCCGAAC

CYP6A1

GACACTGTGCATCCGCCTGGTCCAAGCCCCACTGCATCATCAACGATCCAGCACCTTTTCCTTGGAAATCCGGATCTGTAGCGACGATTTCAAGATCTGCAGT
GTGGCATCAACTACTCCTCCAGCCACGATCAAAGCCGAAACTCCAGAGAACTTACACCAGTGGCCTCTACTTCCCATCAAGTCTCGATGTGCTCTCGCCCACG
CTCCAAACGTCTCATTACACAAACTCGAATCTGCTCCTTGGGGCC

CYP61

GGTCAAGCGCATCGCAGACGACTACTACATGATTACTGCCGCGCTCGAATTAGTCAACTTCCCCATCATTCTCCCGTACACCAAGACATGGTACGGCAAAAA
GTGCGCCGATAAGGTCCTCGAGGCATTCTCCAACTGCGCTGCCAAGGCCAGAGTCCGCATGAAGCAGAAAGGCGCTGAGCCAGAGTGCATCATGGACCGC
TGGATCACACAAATGATCGAGTCTGATCGTTACCGAGCACGCATTGCCAGCGGCGAAAATGTACCTGCCGAGGAGAAGCCAGCAATGCTCCTCCGCAACTT
CTCCGAT

p6U10-RNAi-Sm-dcl

DCL-1

TTCGCTCAAGCAGACTGATCCCATACCAGAAGACGCCAACAAAGGCAAGCATGGCAGTTCAATCTTGGCGTATAGCGTCAGCCTGTGGAAGAAGTCTCGCT
CAAAGTTCACGTACGCGGAGAATCAGCCAGTCATCGAGACGCAGTTAGCAATTTTGCGCCGTAATATGCTGGCACCGCCAGAGAAGAAAGAAGTCGAGGG
AATCACCAAAGCCTACGTGTGCCCGGAGCTCCTCAAGTTCTCTGCGCTCACACCAGAGATTGCCACTTCCTGCATCGTGTGGCCATCCATTATCCACCGATTT
GAGTCGTACCT

DCL-2

TGGTCAACAGTCACCTCCTAGGGTACTGCTGTTTACGATATTATATCAATCAAGAGATGTTTGACATTGTGCAGACTACCTCTGGAAATTATGACAGTGTGTC
TGCGCGGCGGAAGACACACTTATACGAGTTCATGCGTGCTGGAGCACAGGTGAACAATATCACGTGTCAGGCGGTTGAGCATTTCCACGAGTGCTCTTCGC
AGATTGAGAAGGCACTCGCACATGGCATCGAATATCCTTGGGTCGAGCTGGTTACACTATCACCTCCCAAATTCTTCTGTGACCTGGTCGAGTCTA

p9U10-RNAi-GUS

GUS

CACCCAGGTGTTCGGCGTGGTGTAGAGCATTACGCTGCGATGGATTCCGGCATAGTTAAAGAAATCATGGAAGTAAGACTGCTTTTTCTTGCCGTTTTCGTC
GGTAATCACCATTCCCGGCGGGATAGTCTGCCAGTTCAGTTCGTTGTTCACACAAACGGTGATACGTACACTTTTCCCGGCAATAACATACGGCGTGACATC
GGCTTCAAATGGCGTATAGCCGCCCTGATGCTCCATCACTTCCTGATTATTGACCCACACTTTGCCGTAATGAGTGACCGCATCGAAACGCAGCACGATACGC
TGGCCTGCCCAACCTTTCGGTATAAAGACTTCGCGCTGATACCAGACGTTGCCCGCATAATTACGAATATCTGCATCGGCGAACTGATCGTTAAAACTGCCTG
GCACAGCAATTGCCCGGCTTTCTTGTAACGCGCTTTCCCACCAACGCTGATCAATTCCACAGTTTTCGCGATCCAGACTGAATGCCCACAGGCCGTCGAGTTT
TTTGATTTCACGGGTTGGGGTTTCTACAGGACGTAACCTTAAGACCCGGGA

Supplementary Figure S2. RNAi constructs. **A,** *Populus trichocarpa* (SLMB-28-1) was transformed with vectors containing inverted repeat *CaMV35S* promoters (P35S) that drive constitutive expression of sense and antisense transcripts to form dsRNA and are terminated by dual *CaMV35S* terminators (T35S). p9U10-RNAi-Sm-CYP51 targets *S. musiva* cytochrome p450 lanosterol C- α -demethylase *(CYP51*) and two of its homologs while p6U10-RNAi-Sm-DCL targets both *S. musiva* dicer like (*DCL*) genes.

p9U10-RNAi-GUS targets *E. coli* beta-glucuronidase (*GUS)* and serves as a non-specific dsRNA control. Selectable markers for kanamycin resistance (*NPTII*) and hygromycin resistance (*HPT*) are driven by *Arabidopsis thaliana* ubiquitin promoter (*UBQ10*) and terminated by *CaMV35S* terminator (T35S). **B,** RNAi inducing sequences from fungal target genes or *GUS* control.

Sm-CYP51

GGGAGACCAGGAAUUUUCUCCGCCUCGCCACCCGCCCCGACAUUCAAGACGAGCUCGUCCAAGAGCAAAAGGACGUGCUCGGUGUCAAUCCCGACGGCACUAUCAAAGA
UGUCAGCUACGAAAAUCUCUCCAAACUCACCCUCCUCGGCCAAGUCGUCCGAGAGACGCUCCGCAUCCACGCCCCAAUCCACUCCAUUCUCCGCAAAGUCAAAUCCCCCAU
GCCCGUCGAAGGCACUCCUUACGUGAUUCCCACCACGCACUCUCUCCCUCGCCGCCCCCGGGGCCACGAGCCGAAUGGAUGAACACUUUCCCGAACGACACUGUGCAUCCG
CCUGGUCCAAGCCCCACUGCAUCAUCAACGAUCCAGCACCUUUUCCUUGGAAAUCCGGAUCUGUAGCGACGAUUUCAAGAUCUGCAGUGUGGCAUCAACUACUCCUCCA
GCCACGAUCAAAGCCGAAACUCCAGAGAACUUACACCAGUGGCCUCUACUUCCCAUCAAGUCUCGAUGUGCUCUCGCCCACGCUCCAAACGUCUCAUUACACAAACUCGA
AUCUGCUCCUUGGGGCCGGUCAAGCGCAUCGCAGACGACUACUACAUGAUUACUGCCGCGCUCGAAUUAGUCAACUUCCCCAUCAUUCUCCCGUACACCAAGACAUGGU
ACGGCAAAAAGUGCGCCGAUAAGGUCCUCGAGGCAUUCUCCAACUGCGCUGCCAAGGCCAGAGUCCGCAUGAAGCAGAAAGGCGCUGAGCCAGAGUGCAUCAUGGACC
GCUGGAUCACACAAAUGAUCGAGUCUGAUCGUUACCGAGCACGCAUUGCCAGCGGCGAAAAUGUACCUGCCGAGGAGAAGCCAGCAAUGCUCCUCCGCAACUUCUCCGA
UAAUUCCUGGUCUCCC

Sm-DCL

GGGAGACCAGGAAUUUUCGCUCAAGCAGACUGAUCCCAUACCAGAAGACGCCAACAAAGGCAAGCAUGGCAGUUCAAUCUUGGCGUAUAGCGUCAGCCUGUGGAAGAA
GUCUCGCUCAAAGUUCACGUACGCGGAGAAUCAGCCAGUCAUCGAGACGCAGUUAGCAAUUUUGCGCCGUAAUAUGCUGGCACCGCCAGAGAAGAAAGAAGUCGAGGG
AAUCACCAAAGCCUACGUGUGCCCGGAGCUCCUCAAGUUCUCUGCGCUCACACCAGAGAUUGCCACUUCCUGCAUCGUGUGGCCAUCCAUUAUCCACCGAUUUGAGUCG
UACCUUGGUCAACAGUCACCUCCUAGGGUACUGCUGUUUACGAUAUUAUAUCAAUCAAGAGAUGUUUGACAUUGUGCAGACUACCUCUGGAAAUUAUGACAGUGUGU
CUGCGCGGCGGAAGACACACUUAUACGAGUUCAUGCGUGCUGGAGCACAGGUGAACAAUAUCACGUGUCAGGCGGUUGAGCAUUUCCACGAGUGCUCUUCGCAGAUU
GAGAAGGCACUCGCACAUGGCAUCGAAUAUCCUUGGGUCGAGCUGGUUACACUAUCACCUCCCAAAUUCUUCUGUGACCUGGUCGAGUCUAAAUUCCUGGUCUCCC

GUS

GGGAGACCAGGAAUUCACCCAGGUGUUCGGCGUGGUGUAGAGCAUUACGCUGCGAUGGAUUCCGGCAUAGUUAAAGAAAUCAUGGAAGUAAGACUGCUUUUUCUUG
CCGUUUUCGUCGGUAAUCACCAUUCCCGGCGGGAUAGUCUGCCAGUUCAGUUCGUUGUUCACACAAACGGUGAUACGUACACUUUUCCCGGCAAUAACAUACGGCGUG
ACAUCGGCUUCAAAUGGCGUAUAGCCGCCCUGAUGCUCCAUCACUUCCUGAUUAUUGACCCACACUUUGCCGUAAUGAGUGACCGCAUCGAAACGCAGCACGAUACGCU
GGCCUGCCCAACCUUUCGGUAUAAAGACUUCGCGCUGAUACCAGACGUUGCCCGCAUAAUUACGAAUAUCUGCAUCGGCGAACUGAUCGUUAAAACUGCCUGGCACAG
CAAUUGCCCGGCUUUCUUGUAACGCGCUUUCCCACCAACGCUGAUCAAUUCCACAGUUUUCGCGAUCCAGACUGAAUGCCCACAGGCCGUCGAGUUUUUUGAUUUCAC
GGGUUGGGGUUUCUACAGGACGUAACCUUAAGACCCGGGAAAUUCCUGGUCUCCC

GFP

GUGAGCAAGGGCGAGGAGCUGUUCACCGGGGUGGUGCCCAUCCUGGUCGAGCUGGACGGCGACGUAAACGGCCACAAGUUCAGCGUGUCCGGCGAGGGCGAGGGCGA
UGCCACCUACGGCAAGCUGACCCUGAAGUUCAUCUGCACCACCGGCAAGCUGCCCGUGCCCUGGCCCACCCUCGUGACCACCCUGACCUACGGCGUGCAGUGCUUCAGCC
GCUACCCCGACCACAUGAAGCAGCACGACUUCUUCAAGUCCGCCAUGCCCGAAGGCUACGUCCAGGAGCGCACCAUCUUCUUCAAGGACGACGGCAACUACAAGACCCGC
GCCGAGGUGAAGUUCGAGGGCGACACCCUGGUGAACCGCAUCGAGCUGAAGGGCAUCGACUUCAAGGAGGACGGCAACAUCCUGGGGCACAAGCUGGAGUACAACUAC
AACAGCCACAACGUCUAUAUCAUGGCCGACAAGCAGAAGAACGGCAUCAAGGUGAACUUCAAGAUCCGCCACAACAUCGAGGACGGCAGCGUGCAGCUCGCCGACCACU
ACCAGCAGAACACCCCCAUCGGCGACGGCCCCGUGCUGCUGCCCGACAACCACUACCUGAGCACCCAGUCCGCCCUGAGCAAAGACCCCAACGAGAAGCGCGAUCACAUGG
UCCUGCUGGAGUUCGUGACCGCCGCCGGGAUCACUCUCGGCAUGGACGAGCUGUACAAA

Supplementary Figure S3. dsRNA sequences used in *in vitro* studies. Synthetic double stranded RNAs *Sm-CYP51* (891 bp), *Sm-DCL* (645 bp), and *GUS* (594 bp) were produced by Greenlight Biosciences and are identical to dsRNA produced by RNAi constructs in Fig. S2 minus the restriction sites added between stacked gene fragments, and the addition of flanking 15 bp ITS sequences (blue). GFP dsRNA (714 bp) was transcribed from a reporter construct containing enhanced green fluorescent protein.

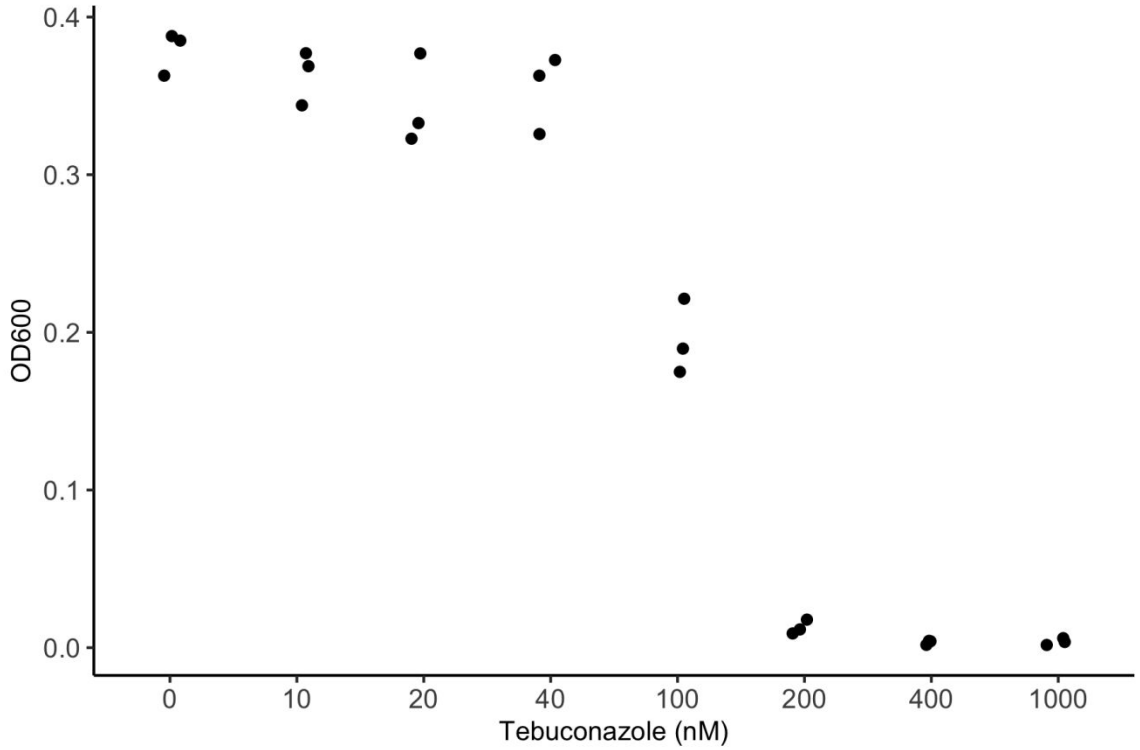

Supplementary Figure S4. Growth of *S. musiva* treated with increasing concentrations of the fungicide tebuconazole in microwell culture. Optical density at 600 nm (OD600) was measured at 4.7 days after treating 10^4 conidia with increasing amounts of Tebuconazole in a total volume of 0.1 ml potato dextrose broth. Data points represent technical replicates from a single experiment. The minimum inhibitory concentration (MIC) of Tebuconazole for *S. musiva* isolate MN-14—defined as the lowest concentration that prevented visible growth—was 200 nM. Tebuconazole and other azole fungicides interfere with the protein product of cytochrome P450 lanosterol C14 alpha-demethylase (*CYP51*) genes.

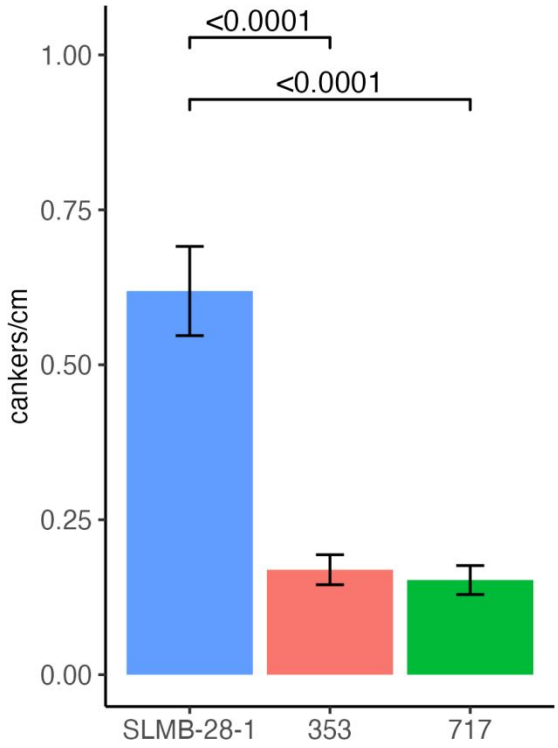

Supplementary Figure S5. Resistance phenotypes of *S. musiva* susceptible and resistant *Populus* clones in a greenhouse spray inoculation. Plants were sprayed to run-off with a $5x10^5$ conidia/ml suspension. Cankers/cm is the mean number of stem cankers formed three weeks post inoculation divided by plant height at time of inoculation. Canker densities for resistant hybrids 353 *and* 717 were lower than susceptible *Populus trichocarpa* clone SLMB-28-1 *(Dunnett's test for multiple comparisons, p-values above brackets).* Error bars show standard deviation.

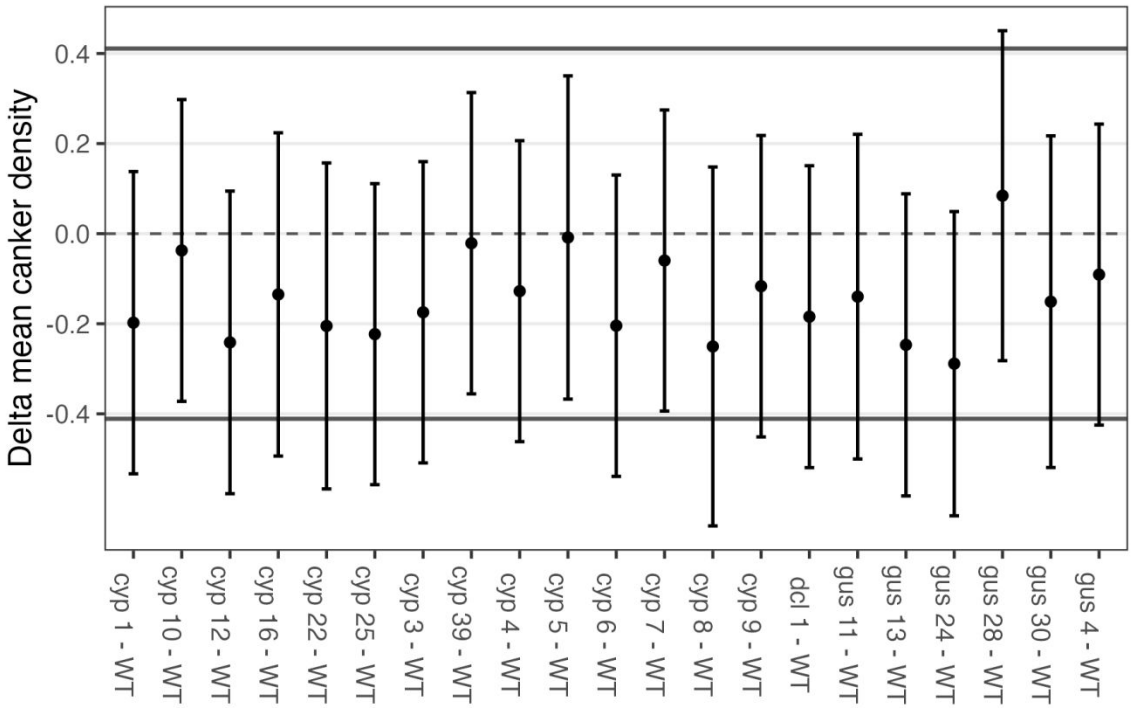

Supplementary Figure S6. Event resistance compared to WT in first greenhouse experiment. Estimated differences in mean canker density between events and *WT*. The hashed horizontal line at zero represents no difference compared to *WT*. Dots show means and error bars are 95% confidence intervals. The solid horizontal bars at +/- 0.411 show the detectable difference in means using a t-test with the observed variation, n=5, 80% power, and alpha = 0.05. Negative HIGS controls are shown on right (gus).

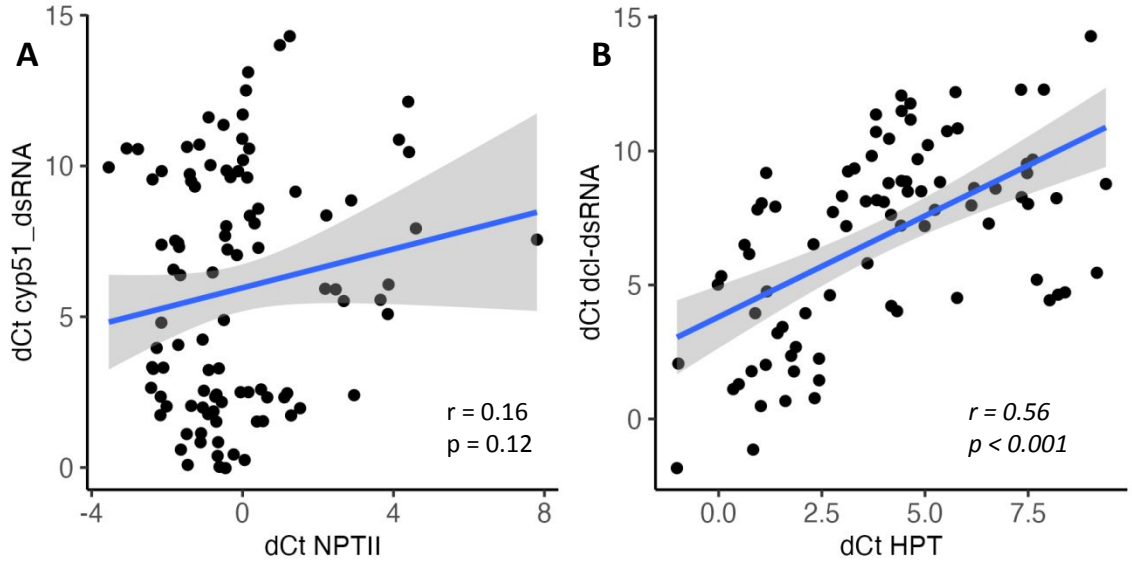

Supplementary Figure S7. Correlation of HIGS transgene and marker gene expression. **A,** Relationship among p9U10-RNAi-Sm-CYP51 events. **B,** Relationship among p6U10-RNAi-Sm-DCL events. Lines are estimated slopes and shading shows 95% confidence.

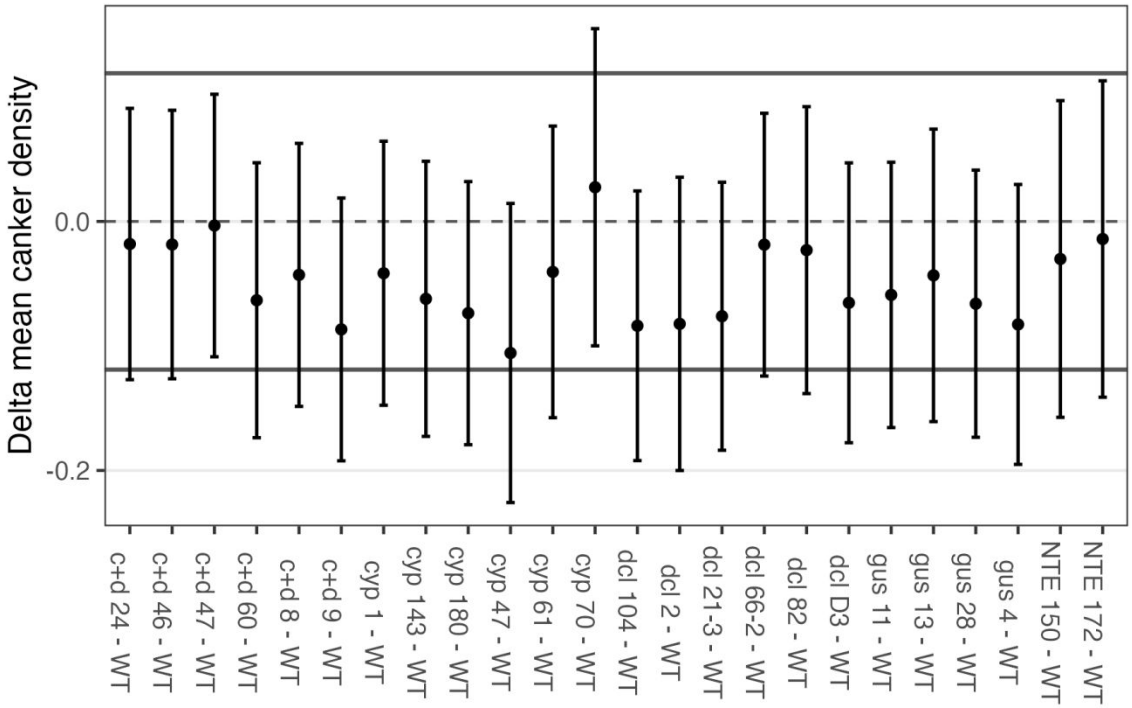

Supplementary Figure S8. Event resistance compared to WT in second greenhouse experiment. Estimated differences in mean canker density between events and *WT*. The hashed horizontal line at zero represents no difference compared to *WT*. Dots show means and error bars are 95% confidence intervals. The solid horizontal bars at +/- 0.119 show the detectable difference in means using a t-test with the observed variation, n=16, 80% power, and alpha = 0.05. Negative HIGS controls and non-transgenic controls are shown on right (gus, NTE).

Supplementary Table S1. List of primers.

Primer name	Primer sequence (5'>3')	Use(s)
Sm-cyp-F1	TTCTCCGCCTCGCCAC	Genotype p9U10-RNAi-Sm-cyp51 transgenic shoots
Sm-cyp-R1	ATCGGAGAAGTTGCGGAG	
Sm-dcl-F1	TTCGCTCAAGCAGACTGATC	Genotype p6U10-RNAi-Sm-dcl transgenic shoots
Sm dcl-R1	TAGACTCGACCAGGTCACAG	
Gus-F	TGTTCGGCGTGGTGTAGAG	Genotype p9U10-RNAi-gus transgenic shoots
Gus-R	TCCTGTAGAAACCCCAACCC	
cyp-ex-F2	TCCCGACGGCACTATCAAAG	Transgene expression of Sm-cyp51 dsRNA
cyp-ex-R2	ACGTAAGGAGTGCCTTCGAC	
dcl-ex-R1	CTCCGCGTACGTGAACTTTG	Transgene expression of Sm-dcl dsRNA
dcl-ex-F2	TCGAGGGAATCACCAAAGCC	
gus-ex-F3	CGTAATGAGTGACCGCATCG	Transgene expression of gus dsRNA
gus-ex-R3	AAGCGCGTTACAAGAAAGCC	
nptII-F	CTTGCCGAATATCATGGTGGAA	Transgene expression of nptII marker
nptII-R	GGTAGCCAACGCTATGTCCTGA	
hpt-F1	TATCCACGCCCTCCTACAT	Transgene expression of hpt marker
hpt-R1	CGACGTCTGTCGAGAAGTTT	
ef1b-F	AACCTGGTCGTGATTTCCCT	P. trichocarpa ef1-beta reference for relative expression
ef1b-R	ATCACCAGCAGCCTCCTTG	
Sm-cyp51-F7	AAAGGAAGACTACGGCTATGG	Expression of S. musiva cyp51
Sm-cyp51-R7	TGCAAATTGCTCTCCAATGC	
Sm-cyp6A1-F2	GATTTCTCCGAAGGCTATGC	Expression of S. musiva cyp6A1
Sm-cyp6A1-R2	GGAAAAGTACATGGAAAAGGC	
Sm-cyp61-F4	TCTCGGTCAGACATATGCG	Expression of S. musiva cyp61
Sm-cyp61-R4	AAAACCTTGATCTCTTCGCTG	
Sm-dcl1-F	GATCCCAGGTATGCCTCACG	Expression of S. musiva dcl1
Sm-dcl1-R	AACTGCCATGCTTGCCTTTG	
Sm-dcl2-F	TCCAGTGACCAGTGTGAAGC	Expression of S. musiva dcl2
Sm-dcl2-R	CGCATCGCATAGTCGGTTTG	
Sm-bt-F3	TCCACCTTCGTCGGAAACAG	S. musiva beta-tubulin referece gene for relative expression
Sm-bt-R3	TCGTCCATACCCTCACCAGT	
Sm-act-F2	TAAGCGCGTACTGCGTAGAG	S. musiva actin referece gene for relative expression
Sm-act-R2	ACTGCCATTCCCATCACTCG	
Sm-bt-F3	TCCACCTTCGTCGGAAACAG	S. musiva beta-tubulin referece gene for relative expression
Sm-bt-R3	TCGTCCATACCCTCACCAGT	
Sm-act-F2	TAAGCGCGTACTGCGTAGAG	S. musiva actin referece gene for relative expression
Sm-act-R2	ACTGCCATTCCCATCACTCG	
GFP-F	GTGAGCAAGGGCGAG	Genotyping L4440-eGFP colonies
L444-R	AGCGAGTCAGTGAGCGAG	
Kpn1-eGFP-F	GATCGGTACCGTGAGCAAGGGCGAG	Cloning L4440-eGFP for in vitro transcription DNA template
BglII-eGFP-R	GATCAGATCTTTGTACAGCTCGTCCAT	

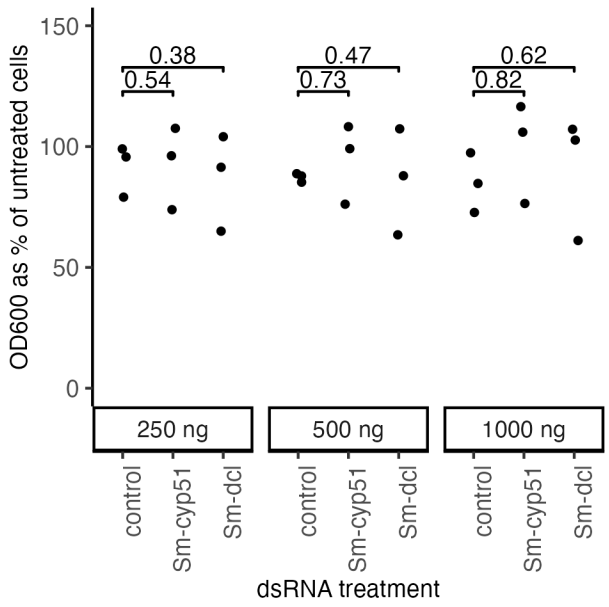
150
100
50
0
OD600 as % of untreated cells
0.38
0.54
0.47
0.73
0.62
0.82
250 ng
500 ng
1000 ng
control
Sm-cyp51
Sm-dcl
dsRNA treatment

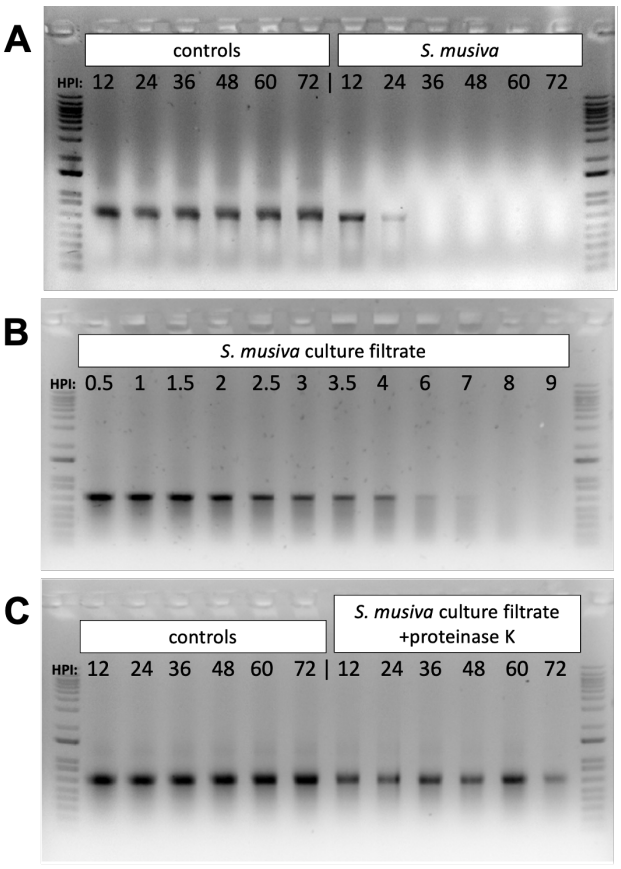
A
controls
S. musiva
HPI: 12 24 36 48 60 72 | 12 24 36 48 60 72
B
S. musiva culture filtrate
HPI: 0.5 1 1.5 2 2.5 3 3.5 4 6 7 8 9
C
controls
S. musiva culture filtrate
+proteinase K
HPI: 12 24 36 48 60 72 | 12 24 36 48 60 72

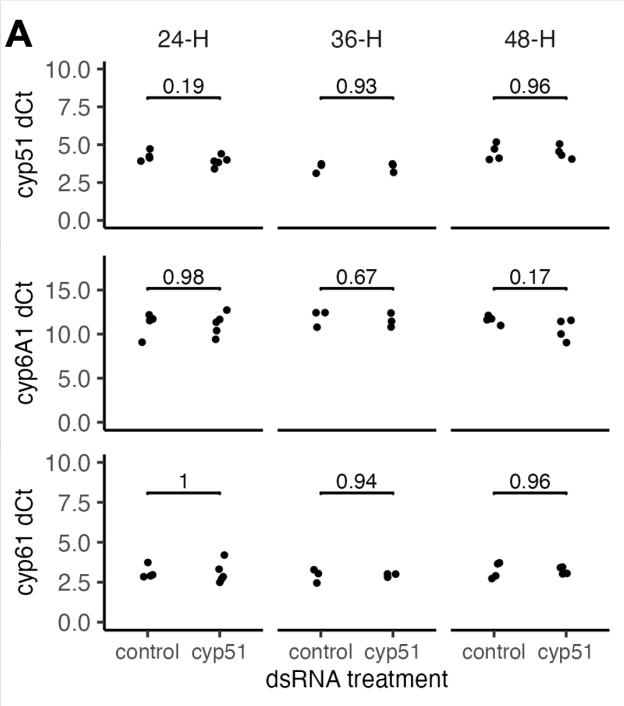
A
24-H
36-H
48-H
cyp51 dCt
cyp6A1 dCt
cyp61 dCt
0.19
0.93
0.96
0.98
0.67
0.17
1
0.94
0.96
control
cyp51
dsRNA treatment

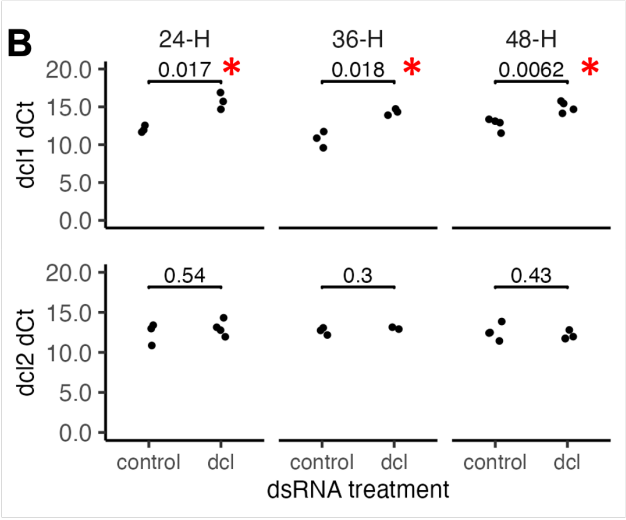
B
24-H
36-H
48-H
dcl1 dCt
dcl2 dCt
0.017
0.018
0.0062
0.54
0.3
0.43
control
dcl
dsRNA treatment

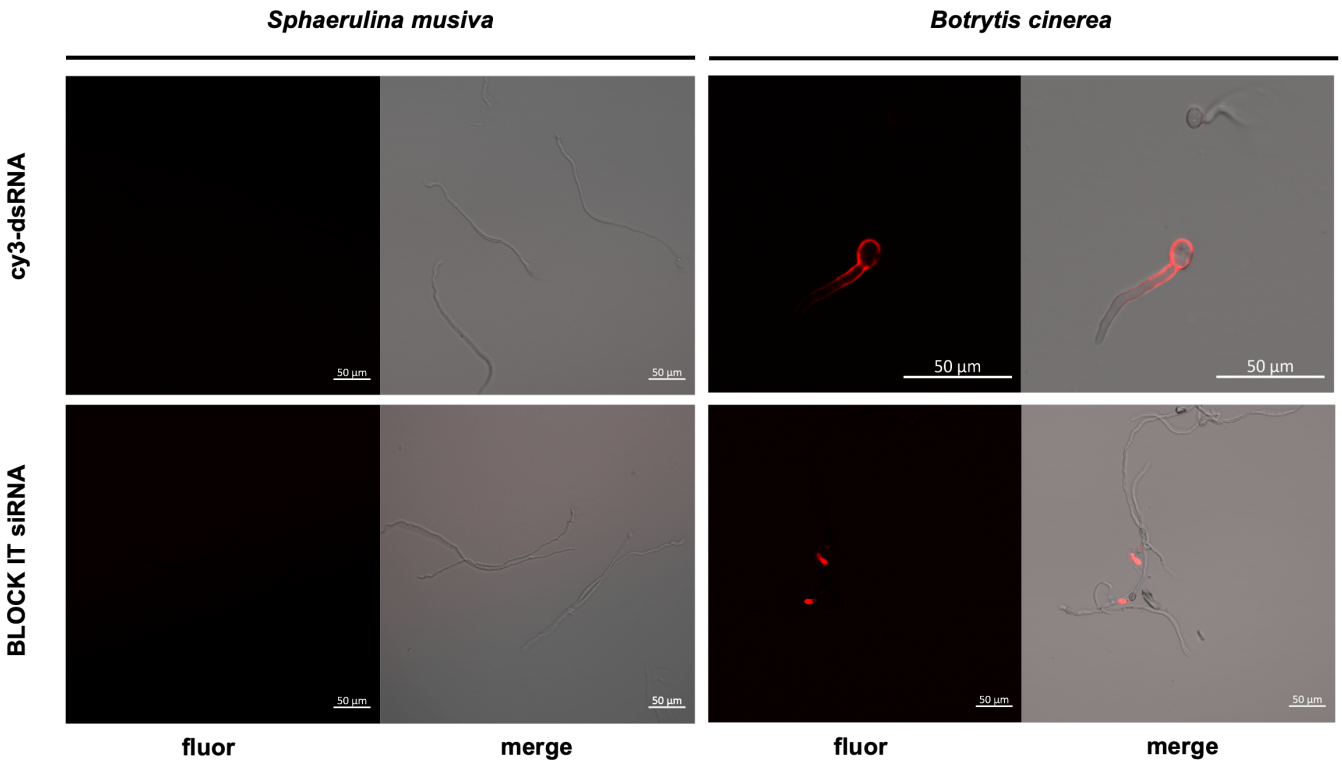
Sphaerulina musiva
Botrytis cinerea
cy3-dsRNA
BLOCK IT siRNA
50 µm
fluor
merge
fluor
merge

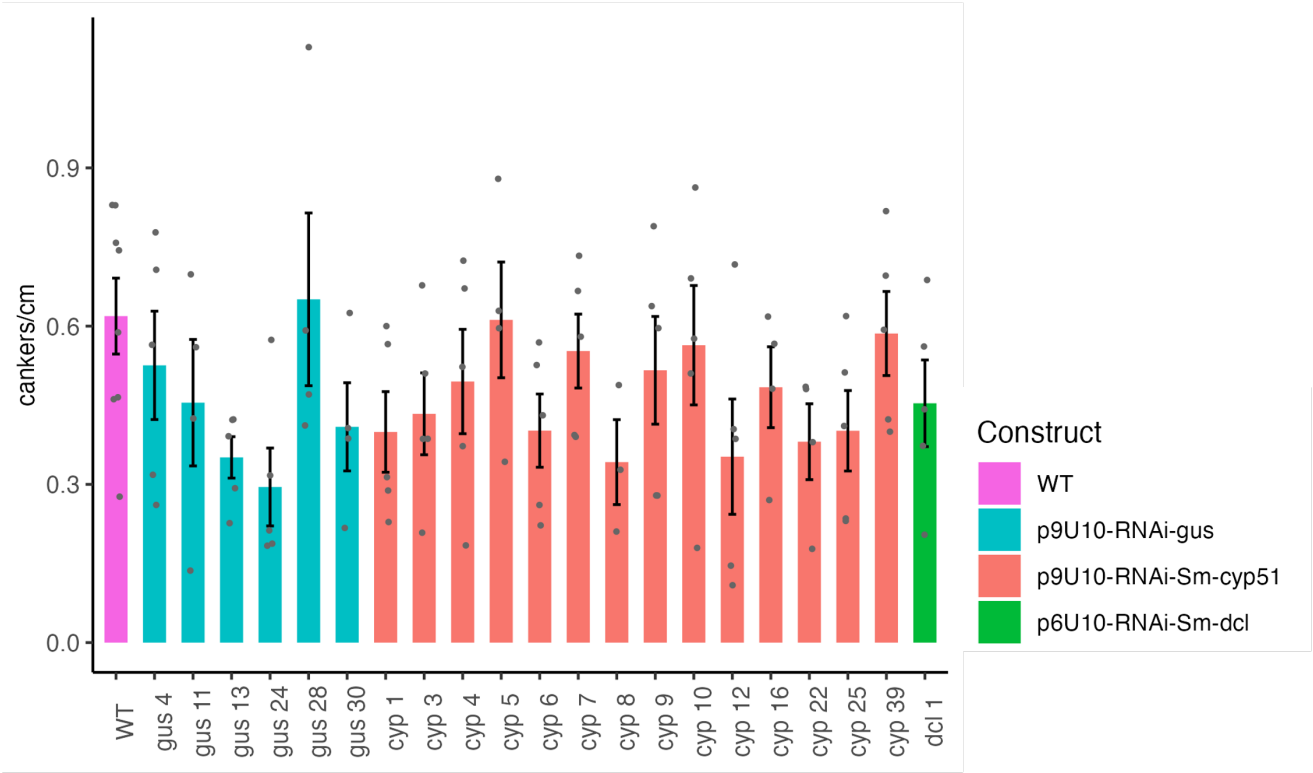
cankers/cm
0.0
0.3
0.6
0.9
WT
gus 4
gus 11
gus 13
gus 24
gus 28
gus 30
cyp 1
cyp 3
cyp 4
cyp 5
cyp 6
cyp 7
cyp 8
cyp 9
cyp 10
cyp 12
cyp 16
cyp 22
cyp 25
cyp 39
dcl 1
Construct
WT
p9U10-RNAi-gus
p9U10-RNAi-Sm-cyp51
p6U10-RNAi-Sm-dcl

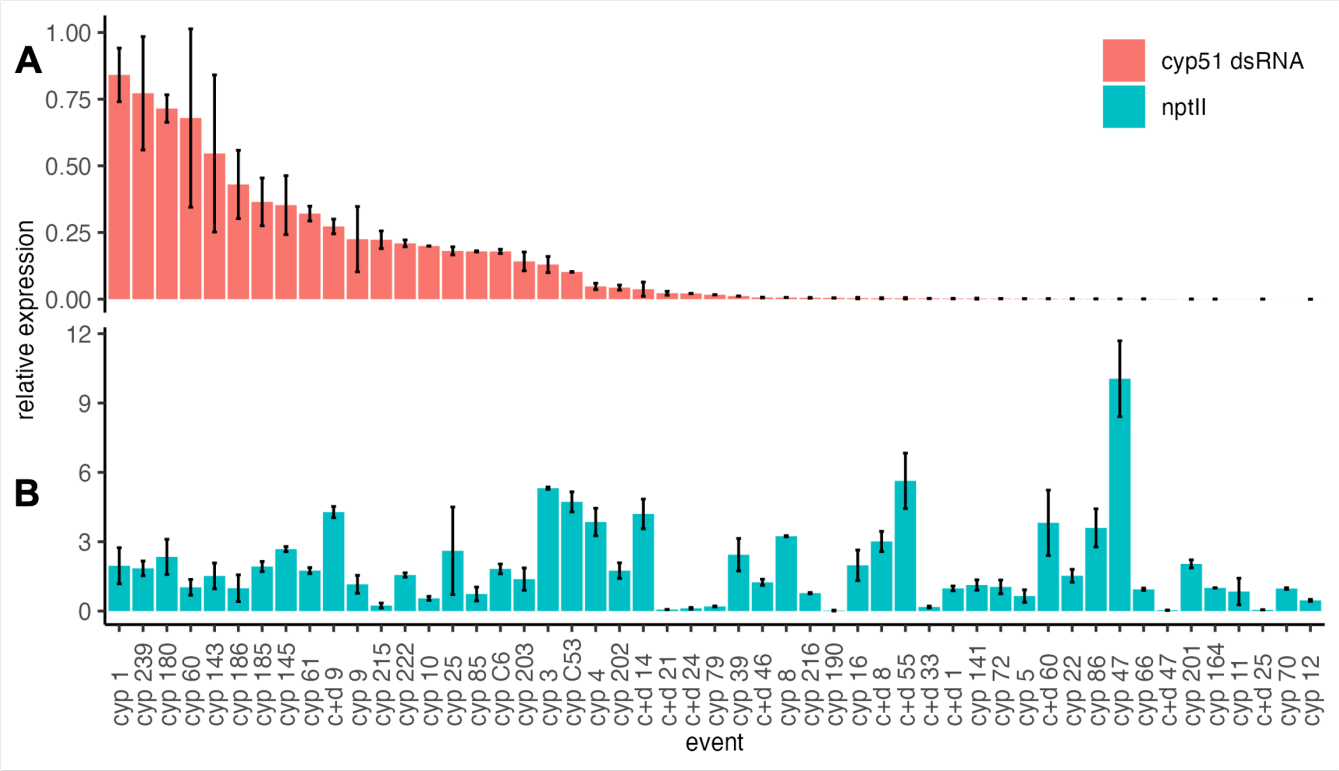
A
B
relative expression
1.00
0.75
0.50
0.25
0.00
12
9
6
3
0
cyp51 dsRNA
nptII
cyp 1
cyp 239
cyp 180
cyp 60
cyp 143
cyp 186
cyp 185
cyp 145
cyp 61
c+d 9
cyp 9
cyp 215
cyp 222
cyp 10
cyp 25
cyp 85
cyp C6
cyp 203
cyp 3
cyp C53
cyp 4
cyp 202
c+d 14
c+d 21
c+d 24
cyp 79
cyp 39
c+d 46
cyp 8
cyp 216
cyp 190
cyp 16
c+d 8
c+d 55
c+d 33
c+d 1
cyp 141
cyp 72
cyp 5
c+d 60
cyp 22
cyp 86
cyp 47
cyp 66
c+d 47
cyp 201
cyp 164
cyp 11
c+d 25
cyp 70
cyp 12
event

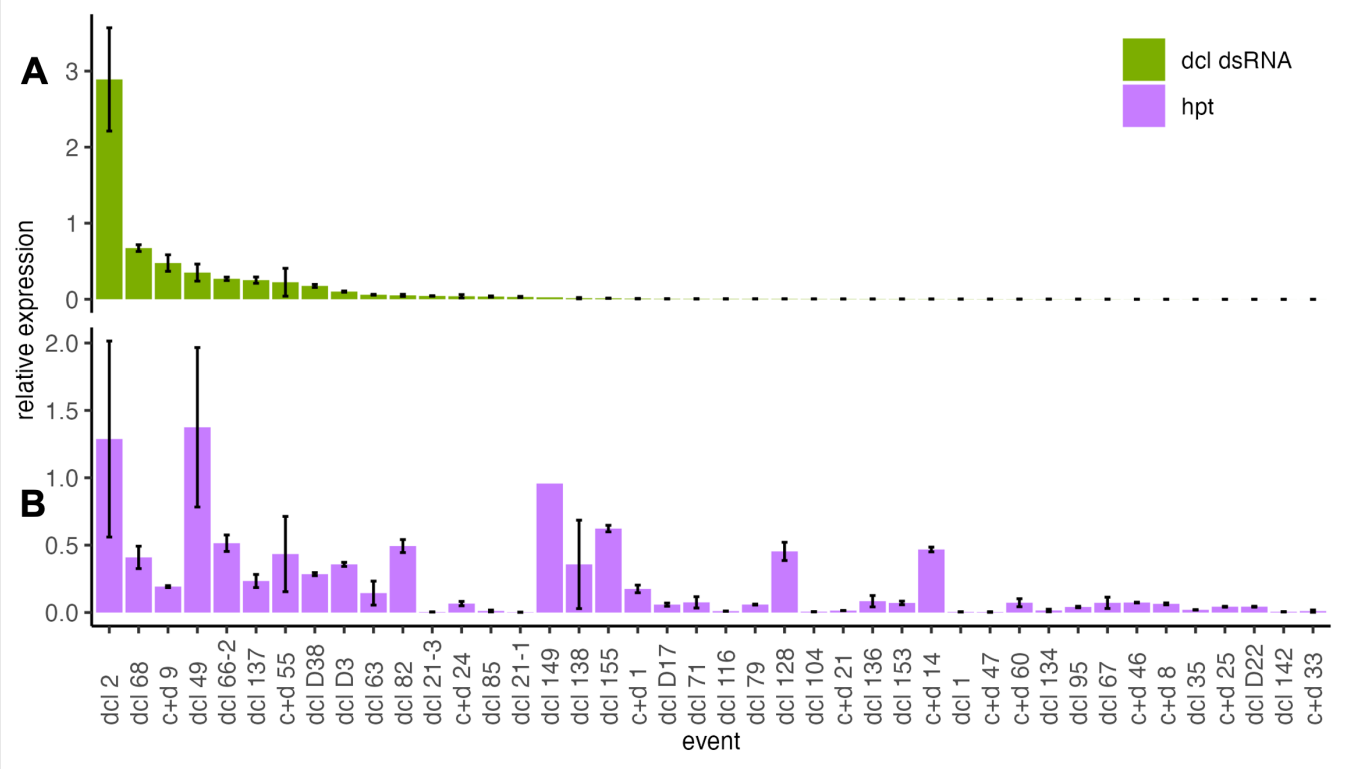
A
B
dcl dsRNA
hpt
relative expression
event
dcl 2
dcl 68
c+d 9
dcl 49
dcl 66-2
dcl 137
c+d 55
dcl D38
dcl D3
dcl 63
dcl 82
dcl 21-3
c+d 24
dcl 85
dcl 21-1
dcl 149
dcl 138
dcl 155
c+d 1
dcl D17
dcl 71
dcl 116
dcl 79
dcl 128
dcl 104
c+d 21
dcl 136
dcl 153
c+d 14
dcl 1
c+d 47
c+d 60
dcl 134
dcl 95
dcl 67
c+d 46
c+d 8
dcl 35
c+d 25
dcl D22
dcl 142
c+d 33

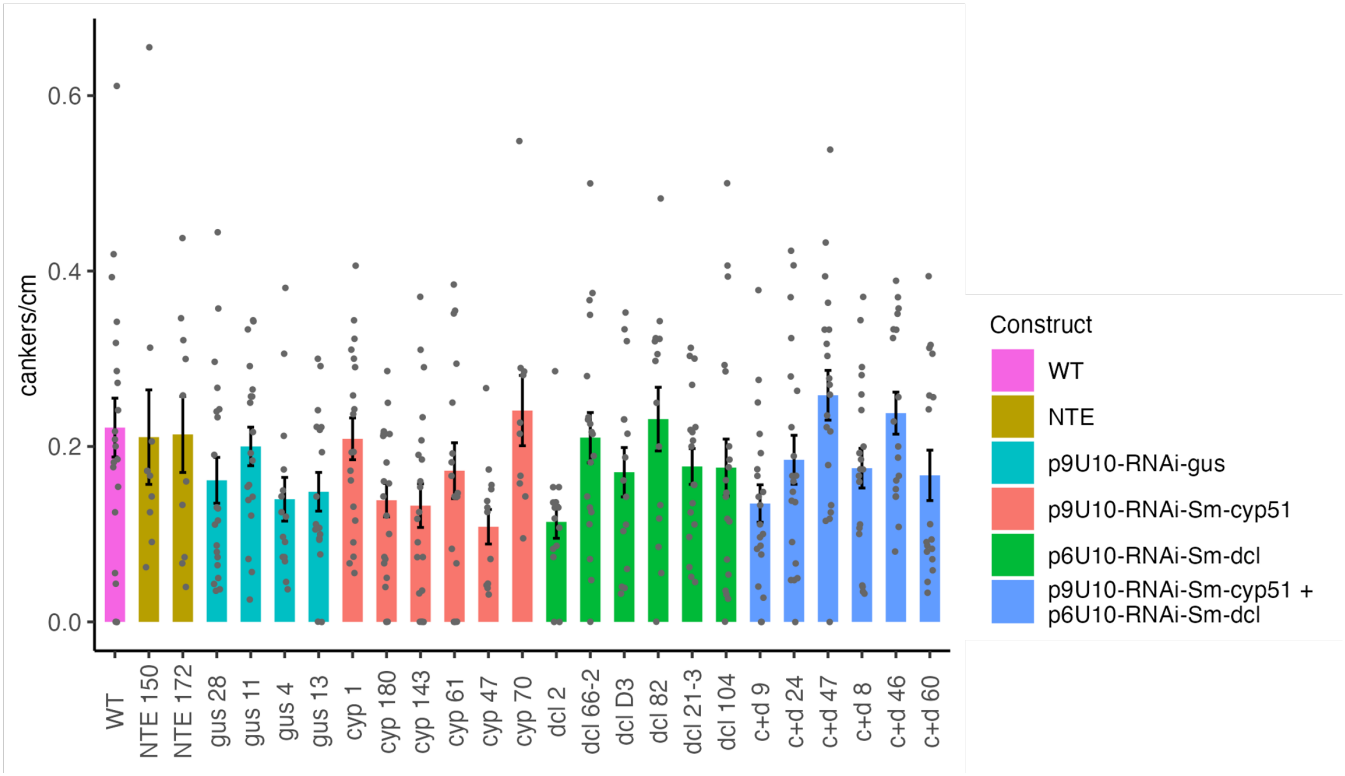
cankers/cm
0.0
0.2
0.4
0.6
WT
NTE 150
NTE 172
gus 28
gus 11
gus 4
gus 13
cyp 1
cyp 180
cyp 143
cyp 61
cyp 47
cyp 70
dcl 2
dcl 66-2
dcl D3
dcl 82
dcl 21-3
dcl 104
c+d 9
c+d 24
c+d 47
c+d 8
c+d 46
c+d 60
Construct
WT
NTE
p9U10-RNAi-gus
p9U10-RNAi-Sm-cyp51
p6U10-RNAi-Sm-dcl
p9U10-RNAi-Sm-cyp51 +
p6U10-RNAi-Sm-dcl

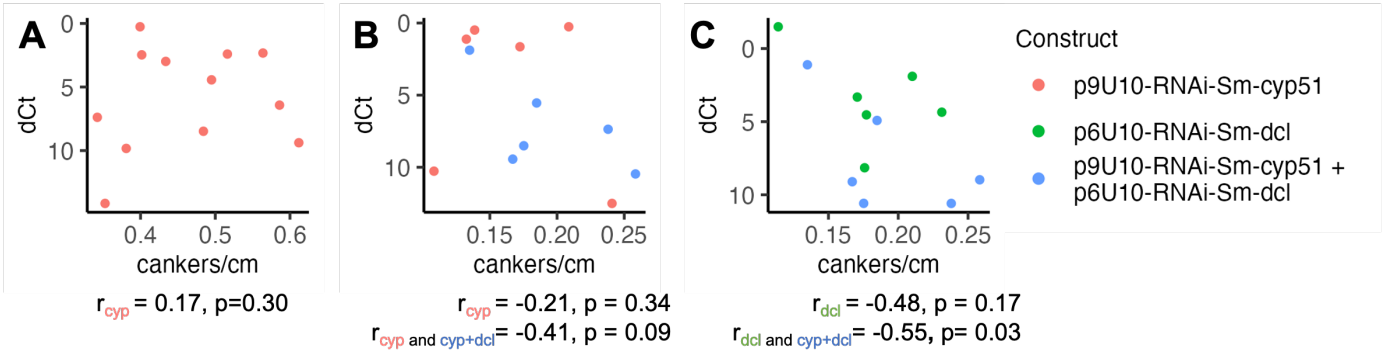
A
B
C
dCt
cankers/cm
0
5
10
0.4
0.5
0.6
0.15
0.20
0.25
Construct
p9U10-RNAi-Sm-cyp51
p6U10-RNAi-Sm-dcl
p9U10-RNAi-Sm-cyp51 + p6U10-RNAi-Sm-dcl
r cyp = 0.17, p=0.30
r cyp = -0.21, p = 0.34
r cyp and cyp+dcl = -0.41, p = 0.09
r dcl = -0.48, p = 0.17
r dcl and cyp+dcl = -0.55, p= 0.03